Carbon-Carbon Composite Closeout Frames for Space Qualified, Stable, High Thermal Conductivity Detector Support Structures.

SBIR Number 55197-99-I
DOE Grant Number DE-FG 03-99ER82802
Phase I Final Report

Eric Ponslet, Franz Biehl, Edward Romero
HYTEC Inc.
5/30/2000

DESIGN ENGINEERING
ADVANCED COMPOSITE APPLICATIONS
ULTRA-STABLE PLATFORMS

110 EASTGATE DR
LOS ALAMOS, NM 87544

PHONE 505 661•3000
FAX 505 662•5179
WWW.HYTECINC.COM

1. **Project Summary**

Space-based high energy particle detectors planned for the near future will not achieve their full scientific goals with the current technology available for space qualified support structures. HYTEC is developing new design and manufacturing approaches that enable the use of advanced carbon-carbon composite materials for those structures.

High-energy particle tracking detectors require ultra-stable, passively cooled, low radiation length, and low mass support structures, for which carbon-carbon composites have uniquely desirable properties. Large, space-based detectors are now being planned for instruments like the Gamma-Ray Large Area Telescope (GLAST). Carbon-Carbon composites have not been used or qualified as primary structural elements for space applications, thus innovative research and development work is needed to achieve this goal.

In this SBIR project, novel manufacturing techniques are experimented with that will allow production of ultra-light, space-qualified thermal/structural elements made of Carbon-Carbon composites. Through fabrication and testing of prototypes, HYTEC is developing and demonstrating a number of key technologies that achieve the thermal and structural goals. These technologies will then be applied in the design, prototyping, and testing full-scale primary support thermo-structures for space-based particle detectors.

In phase I, various design concepts for carbon-carbon support structures were investigated. Numerical modeling was used to evaluate thermal and mechanical performance of those concepts and guide the selection of appropriate composite materials. Prototypes of several key components were produced to evaluate feasibility of the manufacturing approaches. Finally, the most promising concept was selected and its feasibility was demonstrated by building a full size prototype.

In phase II, the concept that was identified and demonstrated in Phase I will be further developed to provide space qualifiable designs. Issues specific to the use of this concept in the space environment will be addressed, leading to a refined design that will be produced and fully tested. Using this technology, a full size prototype of a support structure for the GLAST instrument will be built and tested.

The space qualified carbon-carbon closeout technology that will be developed is directly applicable to the tracker subsystems of the GLAST instrument. It will greatly reduce multiple scattering problems and improve thermal management for that detector. GLAST will become the first, direct commercial application of the new technology. The technology will then be marketed for application in various space–based ultra stable thermo-structures, such as optical benches.

Table of Contents

2. Definitions

- GFRP: Graphite Fiber Reinforced Plastic; any polymeric matrix composite materials reinforced with high performance graphite fibers
- C-C: Carbon-Carbon; a graphite fiber reinforced, carbon matrix composite.
- GLAST: Gamma-ray Large Area Space Telescope[1,2,3].
- MECO: Main Engine Cut-Off.

3. Summary of Phase I Goals, Achievements, and Main Conclusions

The primary goals of the Phase I project were:

- Investigate conceptual design options for carbon composite closeout frames for thermo-structural sandwich panels, using carbon-carbon composites for thermal elements of the design.
- Evaluate the feasibility of the proposed concepts by designing fabrication techniques and procedures, and manufacturing prototypes of key elements of the designs.
- Evaluate key material property requirements for the materials to be used in the design and characterize potential materials.
- Predict the expected performance of the proposed design(s) through numerical simulation of mechanical and thermal behavior.

Our main accomplishments in Phase I can be summarized as follows:

- Several fabrication approaches for composite closeouts were considered and discussed with manufacturers. Of those, two approaches were retained for initial feasibility studies in Phase I. These two approaches are referred to as concepts 1 and 2:
    - Concept 1 is an assembly of molded GFRP components and machined C-C thermo-structural elements. It uses common fabrication techniques and low cost C-C materials. It is assembled by bonding and close tolerances are achieved by machining the critical features on the finished assembly.
    - Concept 2 is based on thin-wall tubular members and machined C-C corner pieces. This concept achieves close tolerances through fixturing at the assembly stage. Various options have been examined for the thermal elements, from ultra-lightweight custom-molded C-C shells with integral heat transfer capability to simpler GFRP tubular shells with co-cured or post-bonded thermal components.
- Material property requirements were derived from thermal gradient requirements based on Finite Element modeling of the two selected concepts. This analysis confirmed the need for high conductivity Carbon-Carbon composite materials.
- An entire, all-composite concept 1 tray prototype was fabricated and clearly demonstrated the feasibility of that concept.
- Various components of concept 2 were fabricated. These include machined 3D C-C corner pieces and heat transfer components and custom molded C-C and GFRP thermal and structural elements.

- We conducted a thorough testing program to evaluate mechanical and thermal properties of low cost 3D and 2D C-C materials widely available from the airplane brake manufacturing industry.
- A detailed Finite Element model of the entire concept 1 tray was created. Numerical simulations were performed to evaluate the dynamic, static, stability, and thermal performance of the proposed concepts.

From the results of the phase I studies, we draw the following conclusions as to the feasibility and promise of the technical approach:

- The feasibility and performance of the first concept has been well established by manufacturing an entire tray. The prototype includes all required features, including bonded metal inserts for threaded connections with the sidewalls. The mass of that prototype tray structure is less than half that of the current baseline design for GLAST. The concept uses relatively low cost materials and fabrication techniques, which should lead to affordable designs.
- Feasibility of the second concept was partially established by manufacturing prototypes of all critical elements. Good quality custom-molded GFRP tubular structural elements and hybrid C-C/GFRP thermal elements were produced.
- More advanced variations on the second concept were experimented with and show some promise. They involve fabrication of very thin walled C-C thermo-structural tubular shells to fulfill both the thermal and the mechanical requirements at a minimum mass. Six prototypes of such shell structures were produced and showed continuous improvement in quality.
- Although both concepts are deemed feasible based on the phase I work, the simpler approach of concept 1 is judged to have better potential to achieve low cost designs and is selected for continued development in Phase II.

4. Carbon Composite Closeout Structures: Motivation and Background

4.1 Summary

Because of their unique thermal conductivity, dimensional stability, and low radiation length, Carbon-Carbon composites have been incorporated as structural and thermal management elements in the design of the ATLAS inner detector for the Large Hadron Collider (LHC). More recently, large area silicon-based particle detectors have been proposed for space-based high-energy detectors such as the Gamma-Ray Large Area Space Telescope[1,2,3] (GLAST). While the unique properties of C-C are still essential to achieving the physics goals in such experiments, the stringent mechanical requirements that characterize space applications introduce new challenges. New efforts are required to develop design approaches and manufacturing techniques that will produce ultra lightweight, high strength, and high reliability Carbon-Carbon thermo-mechanical structures capable of withstanding launch and space environments.

As part of R&D efforts funded by DOE and NASA in the last 4 years, HYTEC conceived of an innovative structural and cooling arrangement for the silicon-based high energy gamma-ray (.01-100 GeV) tracking detector that is part of the GLAST instrument concept (Figure 1).

Through our design studies, we have achieved a compact and passively cooled design concept for a tray, and a method of stacking trays into a tower configuration. Our concept results in a major reduction in the amount of structural material used in the structures and the "dead" area between active tracking regions, thus improving track reconstruction efficiency and background rejection.

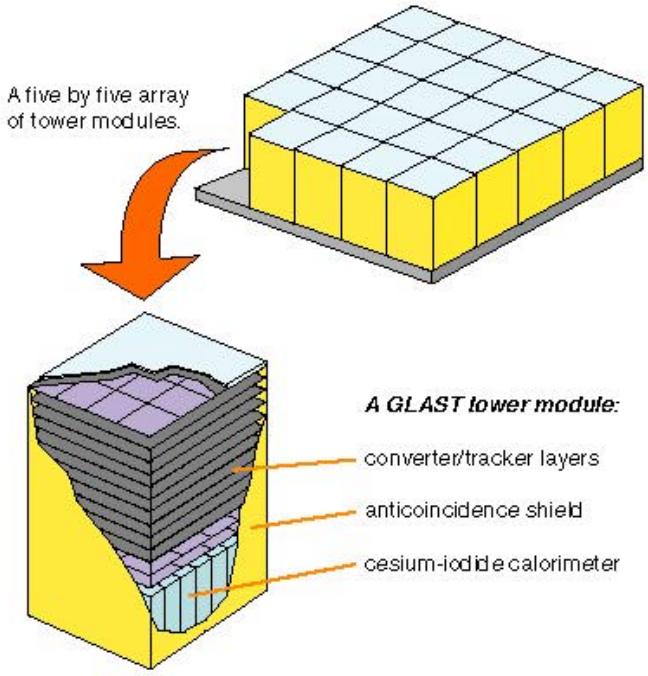

Figure 1: Conceptual layout of the Silicon-GLAST gamma-ray telescope.

A critical component of the concept is a structural and thermal frame that serves as a closeout for the tray's sandwich panel. The closeout has features for aligning and stacking trays into a tower, and must remove the heat generated by front-end electronics mounted on its side. The design of this frame is subject to severe requirements of minimal mass, high thermal conductivity, high dimensional stability and strength, good thermal expansion match to silicon, and minimal interaction with high-energy radiation (i.e. long radiation length). Achieving an ultra-low mass design for this frame is critical to meeting the physics requirements in projects like the Gamma-Ray Large Area Space Telescope (GLAST). Carbon-carbon composites have a number of properties that make them uniquely qualified for this application. However, those materials have never been used in primary structural components for space-based instruments. The launch and space environments impose unique conditions on the design; such conditions do not exist in ground-based detectors where C-C materials have been used or proposed in the past.

4.2 Background

Large area silicon-based particle tracking detectors are being developed for Gamma-ray telescopes like GLAST. The current design philosophy for the GLAST detectors consists of an array of discrete tower modules as shown in Figure 1. Each tower is an independent multi-layer particle-tracking device that integrates its own front-end electronics, mechanical support

structures, and thermal management components. These towers are mounted side-by-side on a support grid that forms the backbone of the instrument and contains an array of calorimeters.

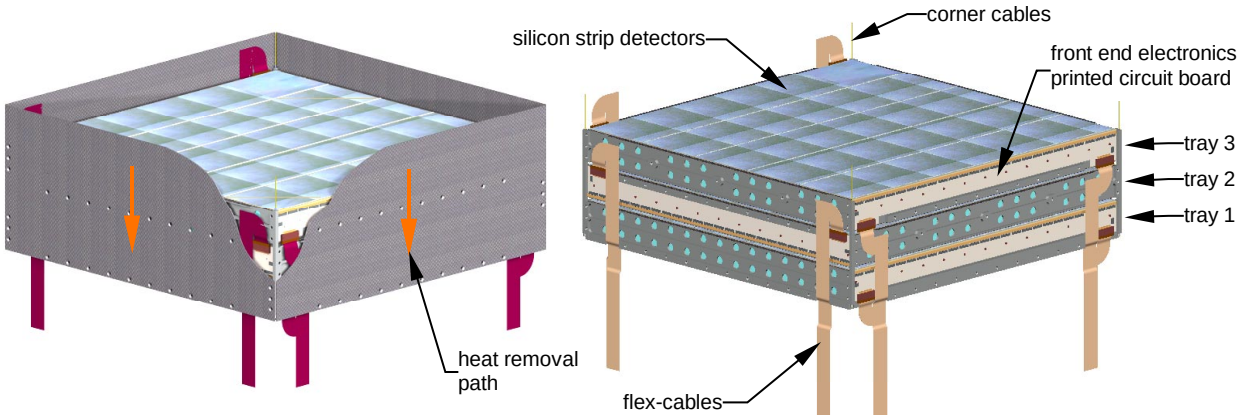

Figure 2: A portion of a stacked tray tower, showing three trays with their front-end electronics PC boards and cabling.

Each tower is itself a stacked assembly of 19 trays, with bolted-on sidewalls for structural reinforcement and passive heat removal. The stacked tray concept developed by HYTEC in earlier DOE and NASA funded activities is illustrated in Figure 2. It is essentially a means of achieving a lightweight and easily assembled support structure for high-energy particle tracking devices using multiple layers of silicon detectors. Each tray (Figure 3) is a self-contained detector module, supported by a sandwich panel with a structural/thermal closeout frame. The top and bottom faces of the tray support printed Kapton bias circuits, thin lead converter layer, and silicon strip detectors. Two opposite sides of each tray serve as mounting surface for front-end electronics PC boards. The waste heat produced by the front-end electronics is conducted through the closeout frame and into the sidewalls, which carry it down to the base of the tower and the instrument radiators.

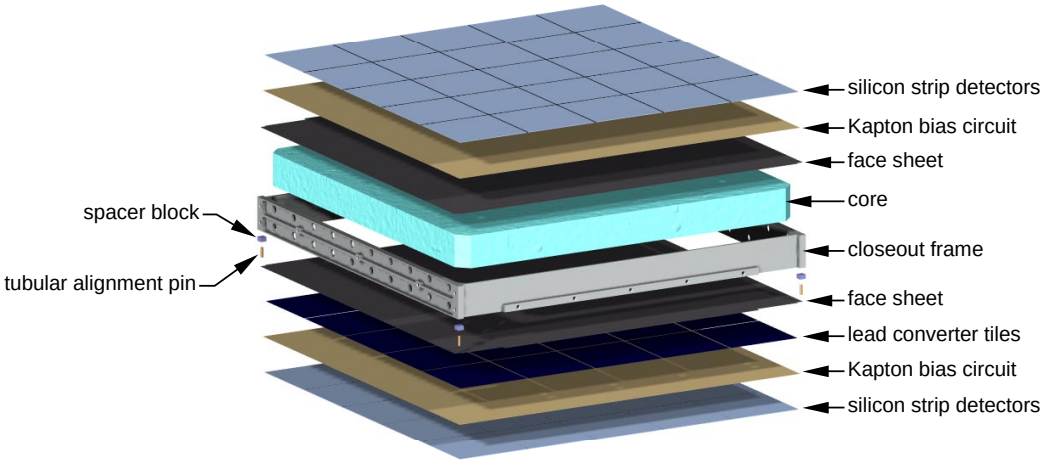

Figure 3: Exploded view of a tray (front-end electronics not shown).

The structure of the tray consists of a lightweight sandwich of carbon composite honeycomb core and high stiffness carbon composite face sheets (Figure 3). This sandwich also incorporates a closeout frame (Figure 4) that serves a number of critical functions:

- It connects the top and bottom face sheets at the edges of the panel and transfers mechanical loads from the tray and its silicon payload into the side walls (which are the primary structural elements for the tower),
- It collects the waste heat generated by the front end electronics and conducts it through a *heat removal boss* (see Figure 4) into the side walls,
- Its corner posts define the vertical spacing of the trays relative to each other; the posts also receive tubular pins for horizontal alignment of the trays,
- The corner posts have holes for threading small diameter synthetic cables through the stack; the cables are tensioned in place and hold the stack together during integration and testing and before assembly of the sidewalls.

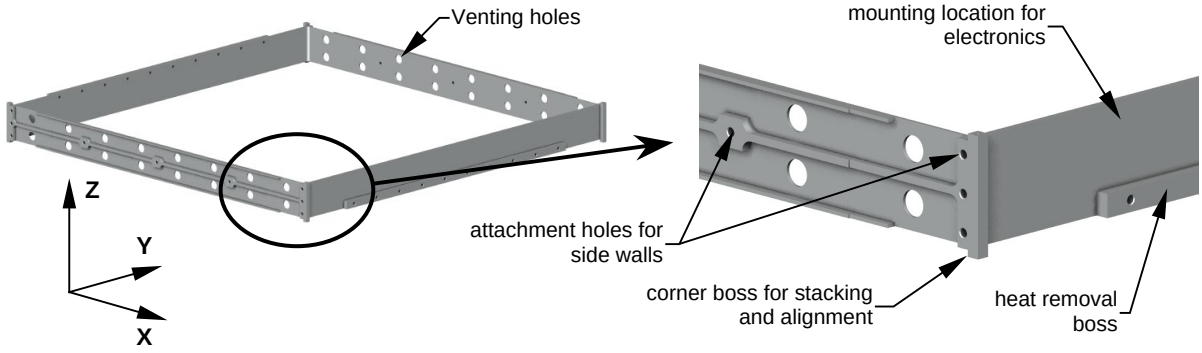

Figure 4: Details of a tray closeout frame (1999 aluminum version shown).

At the end of 1998, HYTEC demonstrated the validity of the stacked tray concept by fabricating a first 10-tray tower prototype (Figure 5) and subjecting it to a series of characterization and qualification structural dynamic tests. These tests demonstrated the validity of the analytical simulation and design approaches. The novel construction concepts, alignment technique, and other key features of the design were corroborated against predictions. The tower was subjected to and survived a series 12.4 g RMS random vibration qualification tests as specified by NASA[15].

In that study, the prototype trays were built around simple, machined aluminum support frames. Little effort was devoted to the selection of optimal material and the minimization of the mass, and more specifically the multiple scattering due to the closeout frame.

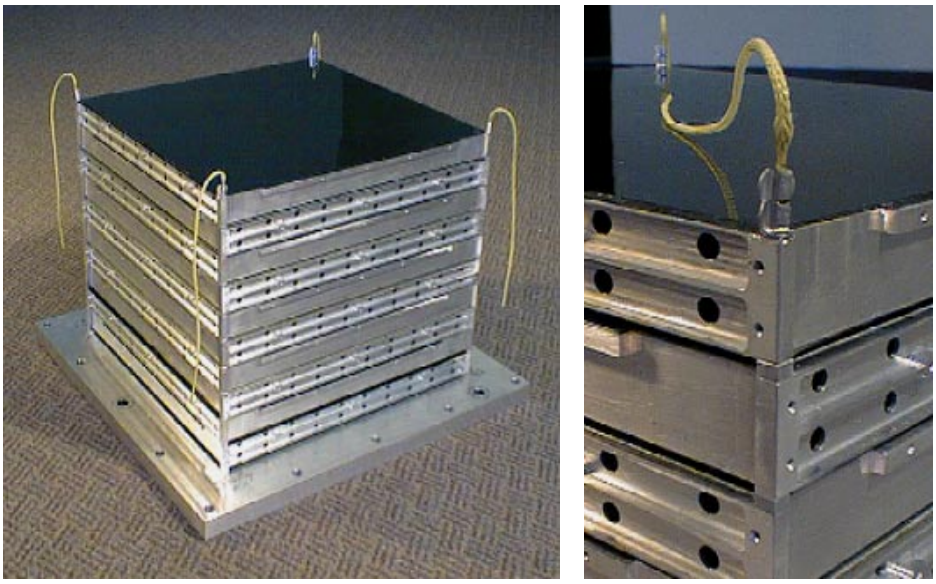

Figure 5: A 1998 aluminum prototype of stacked tray assembly supporting multiple planes of silicon strip detectors for particle tracking experiments.

More recently, in the fall of 1999, an entire functional tracker tower was built using next generation, lighter weight aluminum closeouts, aluminum honeycomb cores, and GFRP face sheets. That tower is shown in Figure 6 and was used in a series of beam tests performed at SLAC in January 2000. The assembly and tests once again confirmed the viability of the stacked tray concept and the dimensional accuracy of the assembled tower.

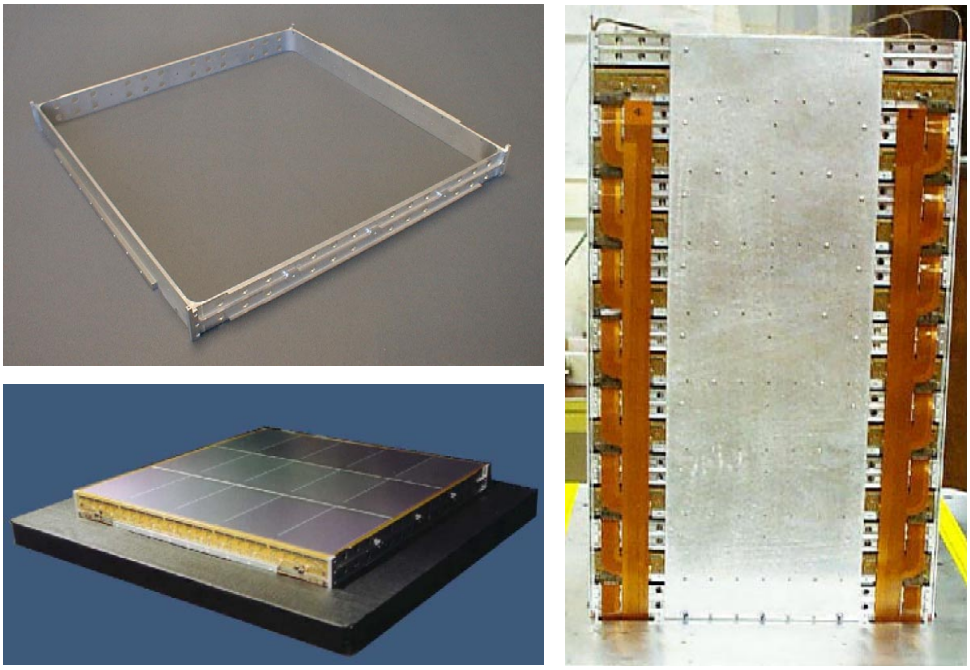

Figure 6: A 1999 functional prototype of tracker tower based on lighter weight aluminum closeouts; right view shows the assembled tower, with live detectors and electronics (with temporary partial coverage side walls).

The beam test tower of Figure 6, however, was still using aluminum for the closeout frames, which because of its high CTE (24×10^{-6}/ºC) relative to silicon (2.6×10^{-6}/ºC) is not a viable flight option.

An individual tray assembly was recently subjected to thermal cycling tests with particular attention to stresses induced in the silicon detector ladders because of CTE mismatch between silicon and other components of the tray assembly (primarily the closeout and the lead converter foils). As illustrated in Figure 7, these tests led to catastrophic failure of a ladder after only a few cycles at relatively modest temperature changes. Two of five detectors in the silicon ladder bonded in the center of tray are severely cracked. Note that with an aluminum closeout, thermally induced stresses are even higher in ladders bonded near the edge of the tray and would lead to failure at even smaller temperature excursions.

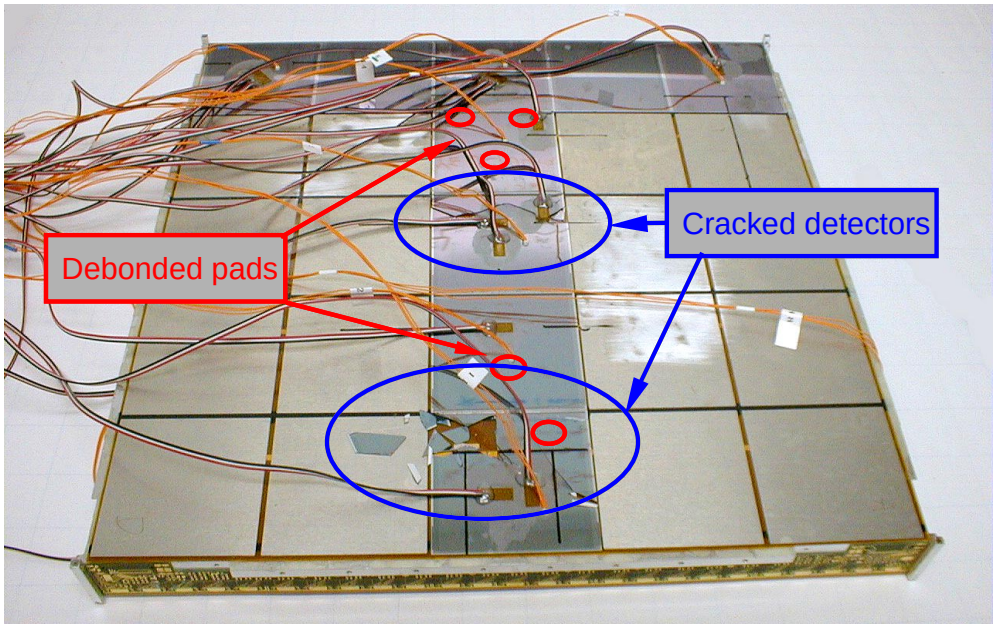

Figure 7: Catastrophic failure of silicon detector ladders caused by CTE mismatch with the rest of the tray assembly (failure occurred after 4 cycles between –55°C and +60°C); broken detectors can be seen at the front and in the center of the ladder.

In the current baseline design of the GLAST tracker tray, a major contributor to the thermal stresses in the ladders is the high CTE aluminum closeout. Figure 8 shows the thermal stress distribution in the ladder direction predicted by a finite element simulation of the tray assembly. Stresses in ladders near the edges are clearly much larger than in center ladders because of the high CTE closeout (note that the test in Figure 7 was representative of an earlier 5x5 design while the model in Figure 8 represents a more recent 4x4 ladder configuration).

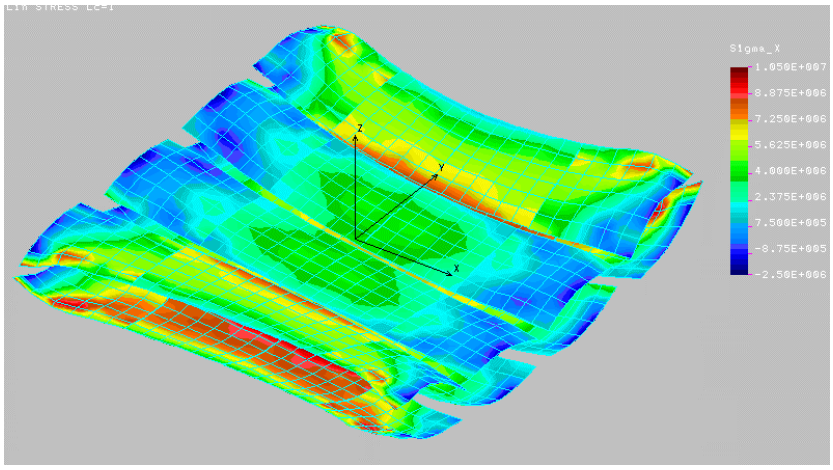

Figure 8: Static CTE-induced response of baseline tray assembly with aluminum closeout to a uniform +20ºC temperature change; for clarity, only the silicon detectors are shown; the color code shows uni-axial stress in the ladder direction (σ_X) in Pascals.

In Figure 9, we compare the thermally induced deformations in a tray assembly built on an aluminum closeout to those in a tray based on an all carbon composite closeout developed in phase I of this SBIR program. The effect of the high CTE aluminum closeout can clearly be seen.

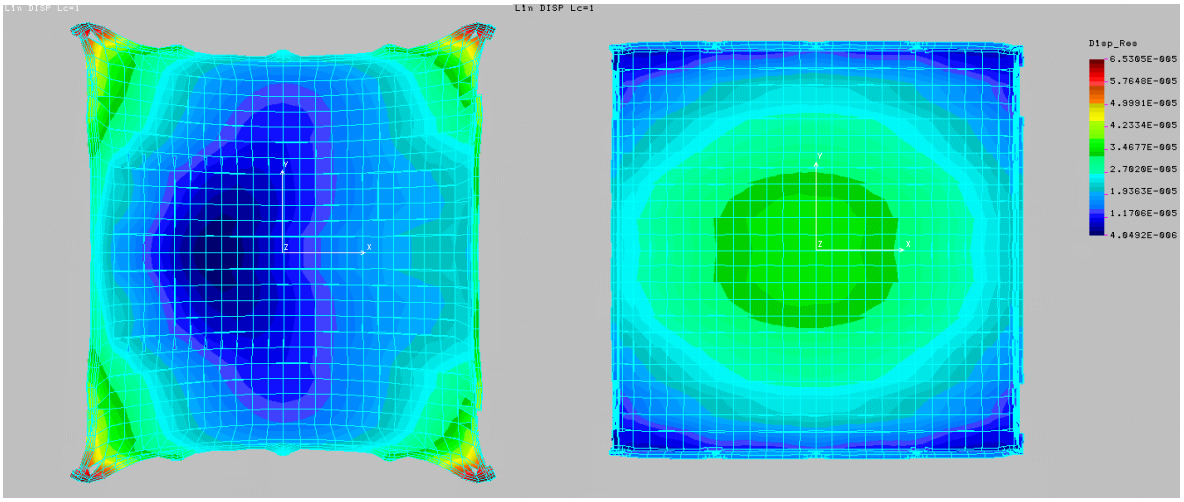

Figure 9: Comparison of static CTE-induced displacements for the aluminum closeout baseline tray (left) and the Concept 1 composite tray (right); the simulation is for a uniform +20ºC temperature change; the scales in the two plots are identical.

For the tray concept to evolve into a viable design for experiments like GLAST, the CTE differentials between different components of the tray must clearly be minimized. In addition, the amount of structural material must be reduced to achieve the physics requirements.

To achieve these goals, advanced materials must be considered that can provide:

- good CTE match with the face sheet and core materials, the silicon detectors, and the side walls,
- high thermal conductivity,
- high stiffness and dimensional stability,
- sufficient strength to survive a launch,
- low outgassing,
- manufacturability in view of the complicated features of the closeout frame, and the very tight dimensional tolerances necessary to achieve the required precision alignment of the trays,
- high radiation length.

Beryllium has been a classical favorite in the high-energy particle detectors, with the longest radiation length and a high stiffness-to-density ratio. However, the significant CTE mismatch between beryllium (11.3×10^{-6}/ºC) and silicon (2.3×10^{-6}/ºC) together with the very high elastic modulus of beryllium would lead to large, unacceptable thermal strains in the detector ladders. Maintaining the precise alignment and relative positioning of the trays for calibration purposes would not be possible. As an indication, the height of a beryllium tracker tower with 17 trays would expand and contract by more than 220 microns under a ±20ºC temperature variation; alignment tolerances for the GLAST trays are about 50 microns. In addition to the thermal expansion problem, beryllium is a hazardous material, requiring extreme precautions in machining which makes it an expensive option.

Resin matrix graphite fiber reinforced composites also have long radiation length and high modulus. However, their thermal conductivity is relatively poor, especially in directions transverse to the fibers. The transverse conductivity of graphite fiber/resin composites is only about 2 W/mºK, compared to 146 W/mºK for Beryllium and more than 30 W/m.ºK for Carbon-Carbon composites. Because of the small, relatively complex features of the tray closeout, it may not be possible to embed fibers in the general orientation of the main thermal fluxes, leading to unacceptable temperature gradients. Resin based composites also have very high CTE in directions transverse to the fibers. Finally, machining of resin-based composites is difficult, particularly when extremely tight dimensional tolerances are required, as is the case for the tray closeouts.

Carbon-carbon (C-C) composites provide the best combination of high thermal conductivity, high stiffness to density ratio, good CTE match with silicon, and no outgassing. The transverse thermal conductivity of C-C is 15 to 40 times better than that of polymeric matrix composites. The properties of C-C, like that of a polymeric matrix composite, are also tailorable. However, its thermal and mechanical properties are more isotropic than those of resin based composites, making it more forgiving in applications with complicated geometry and/or a large amount of machining. Its radiation length (23 cm) is second only to Beryllium (35 cm), and by a small margin to that of polymeric matrix composites (25 cm). It is also very easily machined (in contrast to polymeric matrix composites), and presents no health hazards in this respect.

In view of its unique properties and the unique combination of requirements, C-C is the material of choice for support structures in space-based particle detectors like GLAST.

However, there is limited experience in applying C-C to structural elements and almost no experience when it comes to ultra-lightweight primary C-C structures for space applications.

5. Mechanical, Thermal, and Other Requirements for Tray Closeouts

In developing technological options for all-composite closeouts, we used simplified requirements based on the needs of the GLAST project. These requirements are summarized below:

- Mechanical loading: we only considered two combined pseudo-static launch load factor cases as defined in the GLAST SI-SC IRD document[9], i.e.
  - 4.00gY and 3.35gZ (liftoff & transonic)
  - 0.10gY and 6.60gZ (MECO)
- Other mechanical loads such as vibrations and acoustic inputs were not explicitly considered in Phase I.
- The thermal environment is generally mild, with temperature ranges of -20 to +40°C in survival mode and of -30 to +50°C in qualification testing[10]. Stresses caused by thermal mismatches between components of trays and payload are a major concern, particularly stresses induced in the silicon ladders. To minimize these stresses, all tray and payload components should ideally have CTE's very near that of silicon (about 2.6×10^{-6}m/m°C).
- We require that the thermal conductivity from the PC boards to the sidewall interface be such that the corresponding temperature drop is less than 0.5°C, with a design goal of 0.25°C. This number is based on limits on desired operating temperatures for various GLAST subsystems and allocation of temperature drop budgets between tray closeouts, tower sidewalls, instrument support grid, etc.
- The power dissipated in each PC board is assumed equal to 0.5W; this number is conservative for the baseline GLAST design.
- Qualification for space environment: material selections are limited to those that are or can be qualified for space (i.e. maximum TML of 1% and CVCM of 0.1% per ASTM E595-77/84/90). All major internal air pockets must be vented.
- Particulate contamination is potentially critical in the presence of extremely sensitive detectors and electronics. In particular, the possibility of conductive particle release by carbon composites is a concern. Specific levels and/or testing procedures are not defined at this time.
- Dimensional accuracy and stability: the total positional tolerance budget for the detector strips is about 50 μm. Temperature- or humidity-induced dimensional changes cannot contribute more than a small portion of that budget. The closeout is a potential contributor to this instability, together with face sheets, payload, and tower sidewalls. In addition, machining tolerances for the key alignment features of the closeout must be tight enough to insure proper alignment.
- Stiffness requirements on the closeout itself are relatively mild; tray stiffness is much more a function of face sheet and core selections than closeout design. The closeout should be stiff enough that it does not cause significant drops in tray natural frequencies. This aspect of the design must be addressed at the tray level.

- The fundamental frequency of a tray, as supported in a tower assembly, must be greater or equal to 550 Hz, to avoid the risk of collision between adjacent trays under random vibration excitation.
- Stress levels in the tray closeouts are typically very small (stiffness driven designs), with the possible exception of the bottom tray of the tower where fastener loads may be high. The bottom tray is however an entirely different design and is outside the scope of this program.

6. Examples of Candidate Closeout Materials

A general discussion of material choices for the closeout was presented in Section 4.2 above. Table 1 summarizes typical material properties for a few carbon fiber composites that were considered in the conceptual design phase. Other materials are included for comparison.

material	form	Young's Modulus (GPa)	Radiation Length (cm)	Thermal conductivity (W/mºK)	CTE (10^{-6}/ºC)
3D Carbon-Carbon (Recycled brake disk material)	Thick plates, machinable	30_{XY} / 4_{Z}	23	200_{XY} / 100_{Z}	0.4_{XY} / 4.3_{Z}
K1100 unidirect. / Cyanate Ester	Molded tape layup	540_{X} / low_{YZ}	25	600_{X} / 2_{YZ}	-1.5_{X} / 40_{YZ}
Heat treated quasi-isotropic P30 Carbon-Carbon	Molded tape layup, carbonized and heat treated	200_{XY} / low_{Z}	23	380_{XY} / low_{Z}	-0.9_{XY} / 6_{Z}
6061 Aluminum alloy	various	70	9	180	24
Beryllium	various	318	35	146	11
Silicon Monocrystal	wafers	131	9	150	2.6

Table 1: Typical thermo-mechanical properties of various materials.

Carbon-carbon brake discs for racecars and airplanes are the main industrial application of C-C materials to date. Because of the relatively high volume production, the cost of those materials is very low compared to custom processed C-C. Although they are more porous and not as stiff as custom C-C can be, the mechanical and thermal properties of those materials may be sufficient for at least some components of the closeouts. They were used extensively in fabricating the proof-of-concept prototype in phase I, mostly because of their low cost and short term availability. The properties listed in Table 1 are typical expected values; more details about these materials and actual measured thermo-mechanical properties can be found in Section 9.1.

K1100 unidirectional composites are the highest thermal conductivity carbon composites currently available. Conductivities in excess of 500 W/mK can be achieved in the fiber direction. Mechanical modulus in the fiber direction is also very high. Transverse properties are matrix dominated and typically very poor. Note also that K1100 is one of the most expensive graphite fibers on the market (around $10,000/kg for a resin based, unidirectional prepreg tape).

Heat treated P30 C-C is made from a low cost (about $100/kg for unidirectional prepreg), low-grade pitch based carbon fiber. After carbonization, the composite is subjected to a high temperature graphitization heat treatment, which increases the fiber properties to very near those

of high-end fibers such as P120S (P120 prepreg costs around $3000/kg). This process essentially produces high performance C-C composites from low cost raw materials. The cost of the processing is significant for small quantities but becomes very competitive for larger runs. Another key advantage of this approach is that, because low modulus fibers are used in the precursor, much tighter radii can be molded without risk of breaking fibers.

7. Conceptual Designs for Carbon Closeouts

Several concepts of composite closeouts were considered and discussed with composite manufacturers. Two of those concepts were judged feasible and affordable enough to be detailed and partially or entirely prototyped. The following sections describe those concepts.

7.1 Concept 1: hybrid design with molded GFRP shells and machined C-C bulk pieces

This first concept makes use of the unique properties of C-C materials for the two sides of the tray closeout where high thermal conductivity is needed. The rest of the closeout is based on a thin GFRP "C"-shaped shell. The concept is illustrated in Figure 10.

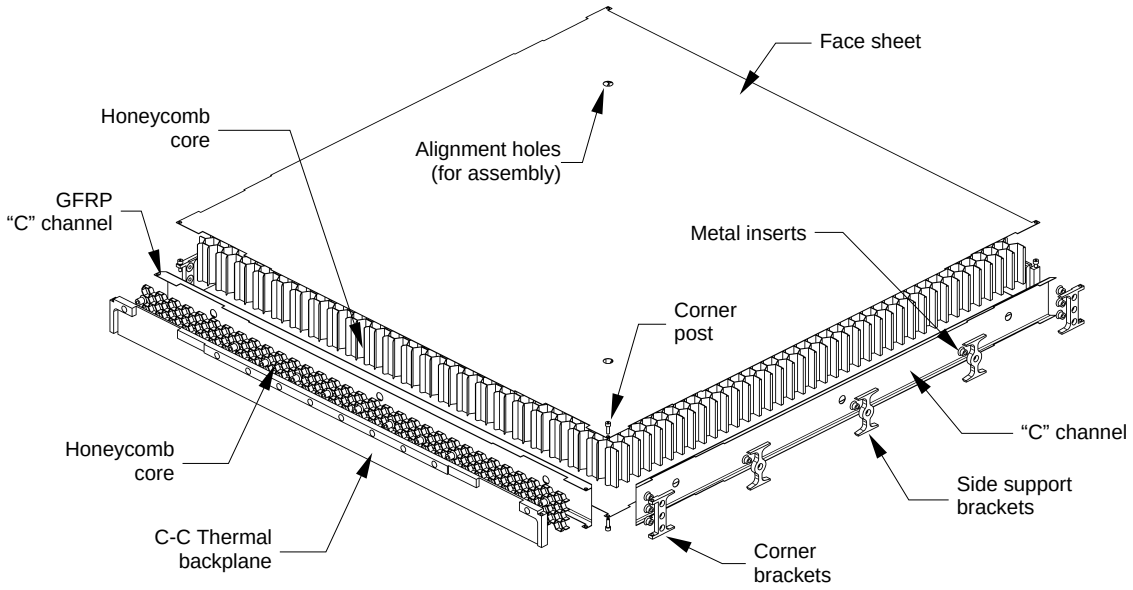

Figure 10: Exploded view of Concept 1 composite tray assembly.

In this concept, the fabrication of the closeout is closely integrated with that of the entire tray: the base sandwich tray is first constructed using core, face sheets, and four thin GFRP "C" channels, with the opening of the "C" facing outward. The rest of the closeout components are then bonded in place within the "C" channels and the entire assembly is machined to finished dimensions. Two sides receive a large, single piece C-C thermal backplane for the PC boards. Those plates are backed by a thin slice of honeycomb core to provide additional stiffness to the assembly during final machining and to insure that the finish machining leaves sufficient bonding areas between the C channel and the face sheets. Those thermal backplanes are also supported at the corners by four corner brackets that are bonded on the other two sides (see detail view in Figure 11). The two non-thermal sides also receive three side brackets for structural

connection with the tower sidewalls. All connections with the sidewalls are done with screws, running through the sidewalls and threaded into metal inserts that are bonded in the thermal backplane and the clips. The inserts are bonded into the composite parts before assembly of the tray but the holes and threads are cut as part of the final machining to insure close tolerances. Also as part of the final machining operations, holes are drilled through the entire tray near the corners and eight metallic corner posts are bonded into those holes. The inserts are then faced and drilled to receive precision tubular alignment pins. Those pins define the alignment of each tray relative to its neighbors.

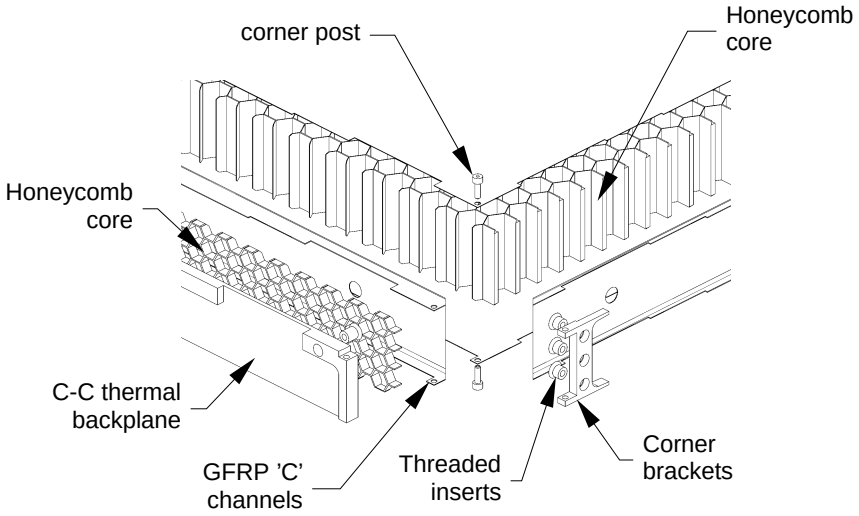

Figure 11: Exploded view of Concept 1 composite tray assembly, close-up on corner details.

The advantages of this approach are that it uses only simple molded GFRP components and C-C parts machined from bulk materials. The costs for materials and components are therefore relatively low. On the other hand, the concept relies on precision assembly using custom alignment and bonding tools as well as fairly extensive machining of the finished tray to provide the high accuracy features required. This labor-intensive approach could make fabrication costs relatively high.

7.2 Concept 2: tubular frame concept

This concept (Figure 12 and Figure 13) is based on a "picture frame" closeout built from molded tubular side members and machined composite corner pieces. The tubes on the two non-thermal sides are thin GFRP shells fabricated by molding around a metal mandrel. The corner pieces are machined from bulk composite blocks with 3D graphite fiber reinforcement. Corner pieces and side tubes receive bonded metal inserts for bolted connections with the tower sidewalls.

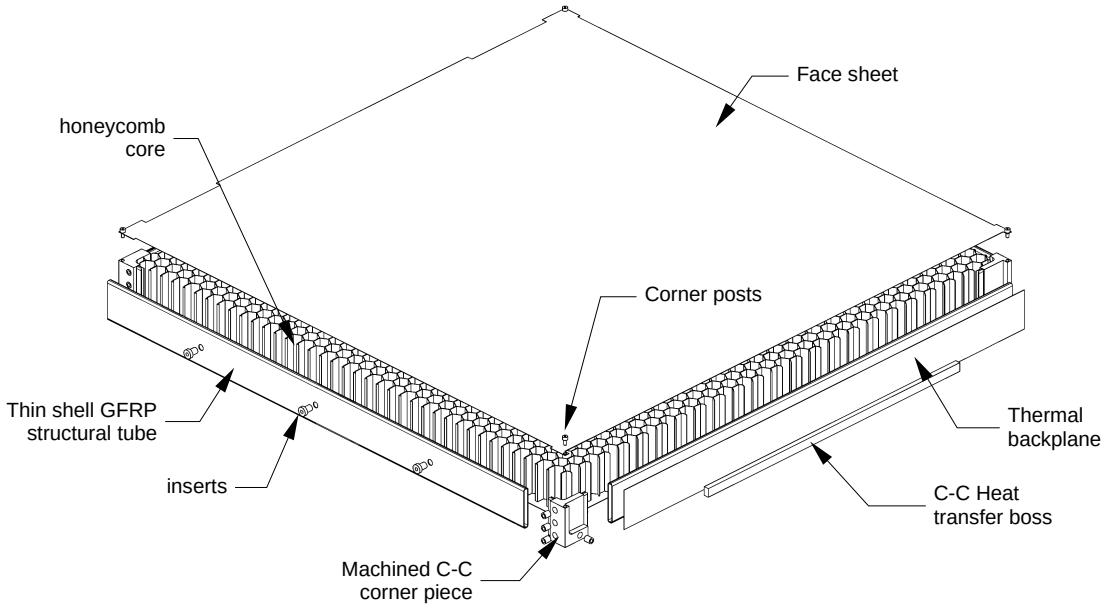

Figure 12: Exploded view of Concept 2 composite tray assembly.

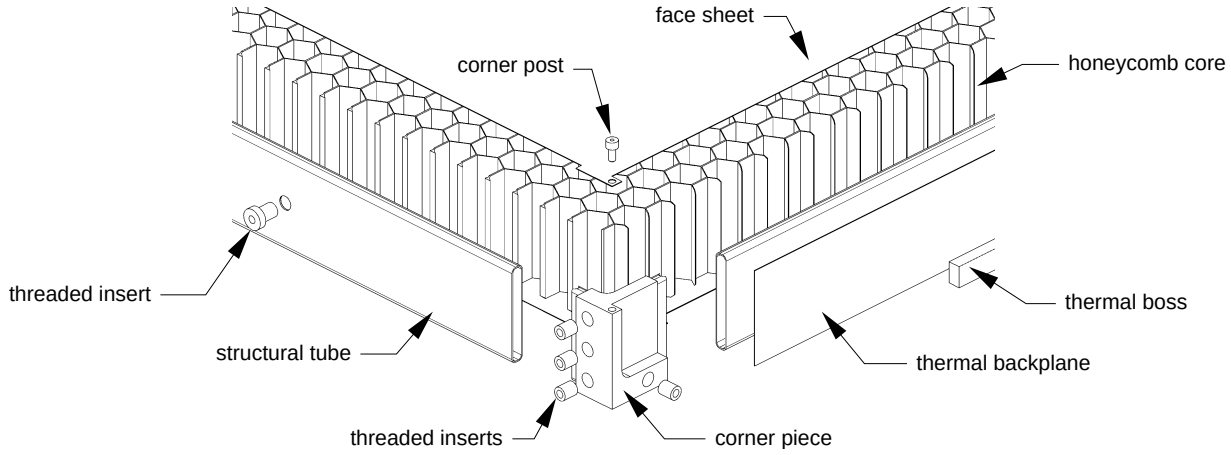

Figure 13: Exploded view of Concept 2 composite tray assembly, close-up on corner details.

Several options were considered for the two thermal sides. Three of these were retained for prototyping; they are illustrated in Figure 14 and will be referred to as 2.a, 2.b, and 2.c.

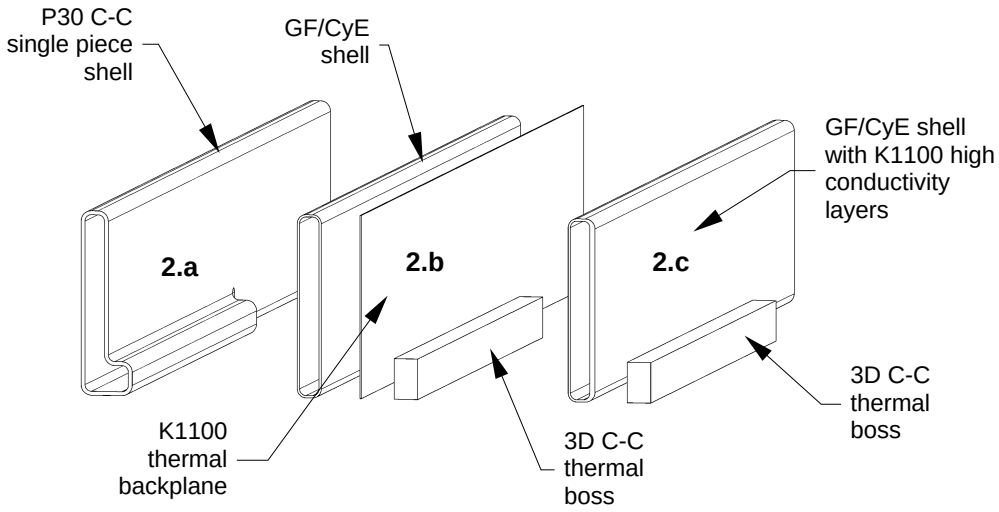

Figure 14: thermal wall options for Concept 2.

The first (and most difficult to fabricate) option consists of a single piece C-C shell with an integral thermal boss. To fit within the required envelope and still provide the necessary thermal contact area with the tower walls, that shell must have very tight inside and outside corners. Such tight radii cannot be molded from high conductivity, high modulus fibers (the fibers would break) so that a resin-based fabrication of such shell is not an option. Instead, a resin-based precursor is molded from low-grade pitch-based P30 fibers then carbonized and heat-treated. The heat treatment increases the thermal and mechanical properties of the fibers to a level comparable to high-end P120 fibers. Because the P30 fibers used in the precursor are very pliable (low modulus), they can be molded around the tight corners without too much difficulty. See Section 9.3.2 below for a description of prototyping efforts.

The second, much simpler approach to fabricating thermal sides for this concept uses a GFRP thin shell tube identical to those used on the two non-thermal sides. A separate high thermal conductivity GFRP thermal backplane is bonded to the outside of one side of the tube to provide a heat removal backplane for the PC board. The thermal boss is machined from bulk C-C material and bonded to the thermal backplane with a thermally conductive epoxy adhesive. The thermal backplane is a thin sheet of ultra high conductivity graphite fibers (K1100) in a resin matrix. Fiber orientations are close to orthogonal to the axis of the tube to maximize heat conduction to the heat transfer boss. Prototypes of this approach were produced without difficulty (see Section 9.3.1).

Finally, the third option is a variation on the last one, where the thermal backplane layers are co-cured with the structural layers of the tubular shell, instead of being added by secondary-bonding. This eliminates an additional step of fabrication but could result in warping of the molded tube as it is cooled down from cure temperatures. Prototypes of this approach were also produced without significant difficulty.

8. Thermal Modeling of Thermal Sides and Derived Material Requirements.

In the previous section, various concepts were described for the thermal sidewalls of the tray assembly. Relatively high conductivity is required in those sides to minimize the temperature drop from the front-end electronics boards to the sidewall interface. In this section, we derive thermal conductivity requirements for the materials used from the temperature drop requirement defined in Section 5 above.

To derive requirements for the thermal conductivities of various materials to be used in the thermal sides of the closeouts, simplified 2-dimensional models of heat transfer from the PC board to the outer surface of the thermal boss were created in the COSMOS[11] finite element package. These models assume that the heat generated by the PC boards is carried through a PC board backing layer, the side of the thermal wall, and into the thermal boss in a 2-dimensional fashion in the XZ plane, i.e. without heat flux components in the Y directions (see Figure 4 for a definition of the axis system. This assumption neglects the effect of the cutouts in the thermal bosses for connector clearance as well as the heat spreading that occurs in angle-ply laminated composites and any heat transfer into the face sheets and/or the two non-thermal sides of the closeout. However, this level of approximation is sufficient to provide approximate requirements for the thermal conductivities of the materials involved in the concepts.

All three models use the following additional assumptions:

- The power dissipated in each PC board is equal to 0.5W; this number is conservative for the baseline GLAST design.
- The boss is assumed to extend all the way across the closeout (i.e. the connector cutouts are neglected).
- The PC board is assumed to have isotropic thermal conductivity equal to 40 W/mK. Note that even though this is not a realistic number for the through-the-thickness conductivity, it does not have any effect on the temperature field in the closeout.
- The PC board to closeout interface is assumed to be made of a thin (0.25 mm) layer of electrically insulating material in intimate contact with both surfaces and with a thermal conductivity of 1 W/mK. Note that modern heat transfer pads for electronics have conductivities as high as 5 W/mK; a lower value is used here to account for imperfect and/or discontinuous contact between the thermal wall, pad, and PC board.
- The outer surface of the thermal boss is assumed isothermal; it was set to 0 ºC for convenience.

As stated in Section 5 above, our design goal is that the temperature drop from the hottest point on the PC board to the outer surface of the thermal boss be smaller than 0.25 ºC. In all three cases, the total temperature drop is dominated by the Z-direction drop in the thermal backplane; temperature drops in bonds and in the PC board backing layer represent less than 20% of the total.

Simulations were first performed with isotropic materials to bracket the thermal conductivities required and lead the preliminary choice of candidate materials. More realistic analyses, using orthotropic thermal properties were then used to set more precise requirements on those properties. The approximate thermal conductivity requirements derived from those

studies are summarized in Table 2. The analyses for the three concepts are summarized in the following sections.

concept		component	required thermal conductivity W/mK	thickness assumed mm
1	Single piece machined CC	CC bulk material	75 in plane, 50 through-thickness	1
2.b or 2.c	Two piece bonded backplane and boss	thin backplane adhesive thermal boss	250 in-plane, 1 through-thickness 1.4 75 in plane, 50 through-thickness	0.250 0.075 -
2.a	Single piece molded CC shell	CC laminate	220 in plane, 30 through-thickness	0.500

Table 2: Approximate thermal conductivity requirements for various thermal wall concepts.

8.1 Concept 1: 3D CC machined thermal backplane

The 3D CC thermal backplane is a monolithic piece, machined from resin impregnated 3D CC material. The FE model is illustrated in Figure 15.

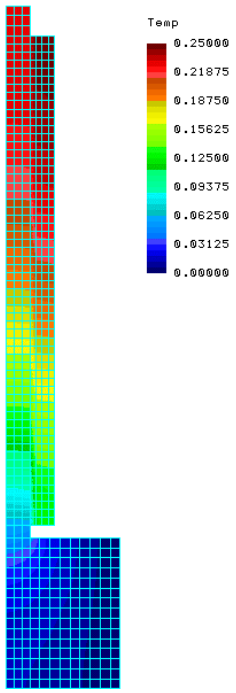

Figure 15: Concept 1: 2D solution for temperature drop between PC board and thermal boss, with K_x=50, K_z=75 W/mK; temperatures in °C.

The back wall thickness was set to 1.0 mm, considered a minimum for machining the part out of bulk CC. 3D CC is produced in large quantities for airplane brake discs. In those materials, the fiber volume content is about isotropic in plane but lower in the through-the-

thickness direction. This produces a ratio of in-plane to out-of-plane thermal conductivities of about 3/2. For a 0.25ºC drop from the hottest point, the approximate required thermal conductivities for the CC material are approximately K_z > 75W/mK (in plane) and K_x > 50 W/mK (through the thickness). Note also that most of the temperature drop occurs along the height of the relatively thin thermal backplane; the drop in the PC board backing layer ranges between 0.015ºC at the top and 0.06ºC at the bottom.

8.2 Concept 2.b or 2.c: two- or three-piece hybrid bonded thermal backplane

This concept would use 3D CC for the heat transfer boss and a thin, molded, high conductivity thermal backplane. The backplane could be made of either CC or GFRP, using high thermal conductivity fibers. The thickness of the backplane was set to 0.25 mm. The FE model is illustrated in Figure 16. Note that backplane was modeled as one wall of the structural tube section. It could also be a separate flat panel, co-cured or post-bonded to the structural element as described in Section 7.2 above.

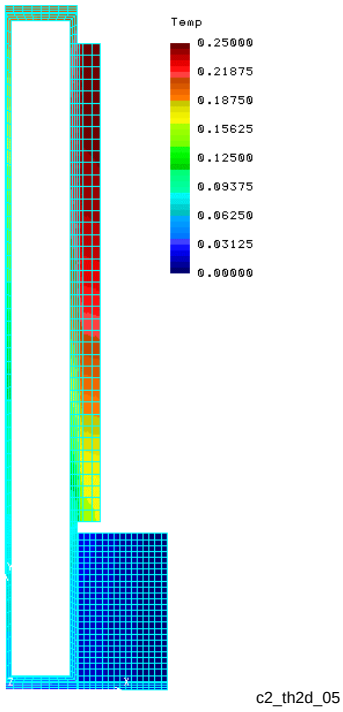

Figure 16: Concept 2.b or 2.c: 2D solution for temperature drop between PC board and thermal boss, with $250_z/1_x$ W/mK thermal backplane, $50_x/75_z$ W/mK thermal boss, and 1.4 W/mK bond; temperatures in ºC.

Figure 16 shows the temperature distribution (from 0ºC at the outer surface of the thermal boss) with the following thermal conductivities:

- Backplane: 250 W/mK in-plane (YZ) and 1 W/mK out-of-plane (X); those values are representative of ultra high conductivity GFRP. Much higher out-of-plane conductivity could be obtained with C-C.
- Thermal boss: K_z=75 W/mK, K_x=50 W/mK, see 8.1 above.

- Adhesive bond between backplane and boss: 1.4 W/mK, typical of modern high thermal conductivity adhesives. The thickness of the bond was set to 75 μm.

Note that the largest part of the temperature drop is again in the thin backplane (i.e. dominated by K_z); the drops in the PC board backing, boss to shell conductive bond, and boss are 0.02 to 0.05ºC, 0.01 to 0.03ºC, and 0.02 to 0.03ºC, respectively.

8.3 Concept 2.a: single piece molded CC Thermal Shell

This concept would use a single piece molded C-C thin shell to carry the heat from the PC board to the sidewall. In this model, a shell thickness of 0.5mm was assumed. The thermal conductivities (along the laminate and through-the-thickness) were adjusted to achieve the 0.25ºC goal for the total temperature drop. The ratio of conductivities in different directions was maintained in a range consistent with 2D C-C layups.

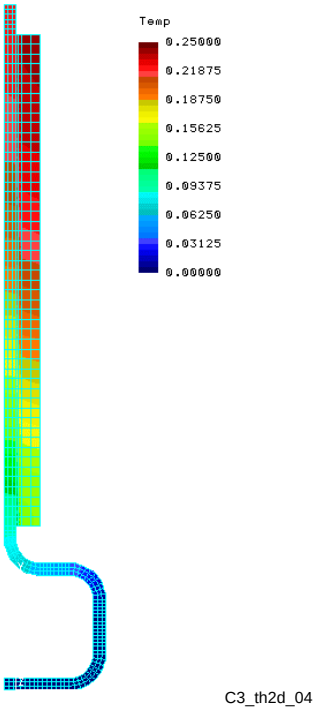

Figure 17: Concept 2.a: 2D solution for temperature drop between PC board and thermal boss, with 220/30 W/mK (along laminate/through-the-thickness, respectively) C-C shell; temperatures in ºC.

Figure 17 shows the temperature distribution through the cross section of the thermal wall for thermal conductivities equal to 220 W/mK in the plane of the laminate and 30 W/mK through the thickness. The temperature at the contact surface with the tower sidewall was set to 0ºC for simplicity. Once again, the bulk of the temperature drop is in the thin backplane; the drop in the PC board backing material tranges from 0.017ºC to 0.048ºC.

9. Prototyping and Test Results

To properly evaluate feasibility of the proposed concepts, several prototype parts and assemblies were produced during phase I. All composite manufacturing and assembly activities were performed by Allcomp, Inc, of City of Industry, California.

9.1 Mechanical and Thermal Properties of C-C Brake Materials

As mentioned in Section 6, airplane brake C-C materials may be useful in the design of composite closeouts as they offer good thermal properties and low CTE at a very low cost. Those materials were used extensively in the fabrication of the proof-of-concept prototype of concept 1. They can be purchased in plate form, between 1/4 and 3/4" thick, and machined into various parts. They are reinforced with quasi 3-directional fiber felts, giving them good thermal properties in all directions. The mechanical properties however are fairly low because of the low grade fibers used, the relatively low fiber volume content (around 25%), and the relatively high porosity. The mechanical strength can be improved by impregnating the brake material with low viscosity resins, which fill the residual porosity, leading to increases in strength.

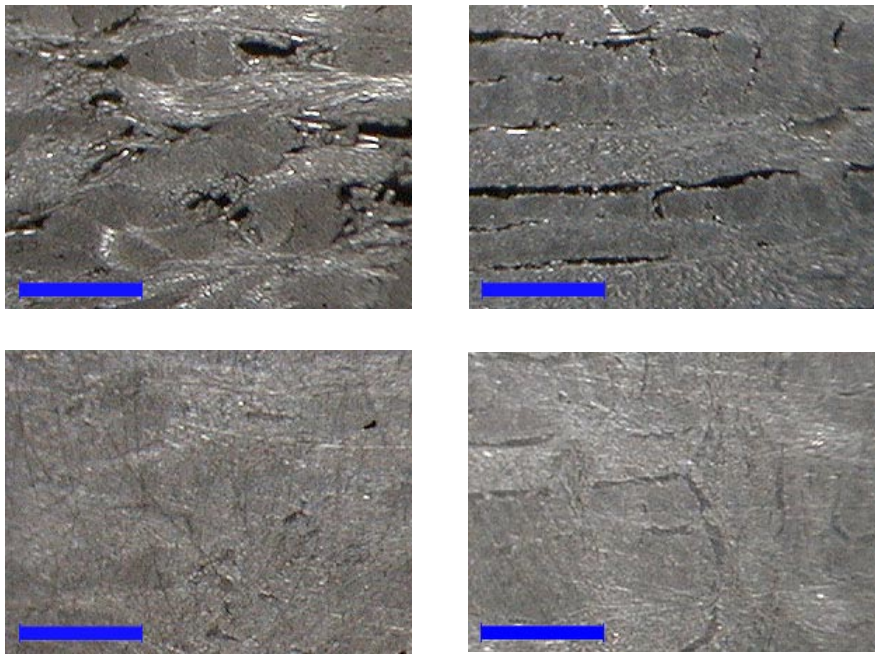

Figure 18: resin impregnation of CC brake materials: micrographs of raw (heat treated recycle brake material) and resin impregnated 2D and 3D CC; the scaling bar in the lower left corner of each view is 1 mm long.

Two types of brake materials were used in the concept 1 prototype. Their thermal and mechanical properties were completely characterized as part of this Phase I project. The two types will be referred to as 2D and 3D materials, although that terminology is maybe somewhat misleading. Both materials were purchased from B.F. Goodrich's Santa Fe Springs facilities in California.

The 2D material is used in Boeing 757 and Lockheed C5B brake discs. It is made from a mostly 2-dimensional (XY) fiber felt, with substantial out-of-plane "waviness" tying the layers together. The 3D material is used for Boeing 777 brake discs and has a more organized fiber distribution made of XY layers "stitched" together with a smaller number of fibers in the Z direction, which give it a slightly higher through the thickness thermal conductivity.

Both materials are first subjected to a high temperature (about 3000ºC) graphitization treatment to increase thermal conductivity and produce micro-cracking in the carbon matrix, opening the pores for resin impregnation. The heat-treated C-C's are then impregnated with a low viscosity resin (Shell Epon 9405/9470) to improve their mechanical strength by sealing the microcracks and pores. Impregnation is performed by back-filling a vacuum chamber with the liquid resin after evacuating air from the C-C pores. The resin is cured at 120ºC (250ºF) then post-cured at 175ºC (350ºF). The resulting resin impregnated C-C's have around 25% fibers, 60% carbon matrix, and 15% resin, by volume.

Figure 18 shows micrographs of the 2D and 3D materials before and after heat treatment and resin impregnation. The pre-impregnation micrographs clearly show large interlaminar cracks and other pores (brake material is not fully densified). Those cracks and pores are at least partially responsible for the poor mechanical properties of low density C-C. Once impregnated, however, the pores and cracks are almost entirely filled with resin, which considerably improves toughness and strength. The resin impregnation also reduces the tendency for C-C materials to release carbon dust, which goes at least part of the way towards qualifying them for space use.

Multiple samples of the resin impregnated C-C materials were sent to testing laboratories for evaluation of thermal and mechanical properties. Stiffness, strength, and CTE measurements were performed by Materials Innovations, Inc. in Huntington Beach, CA. Thermal conductivity measurements were performed by Prof. Hasselman at Virginia Tech (VPI) in Blacksburg, VA. The results of those tests are summarized in Table 3. Properties were measured in three mutually orthogonal directions. Because brake discs (and the fiber arrangements within them) have cyclindrical symmetry, those directions are referred to as radial, tangential, and through-the-thickness.

			2D			3D		
		units	radial	circumf.	through thickness	radial	circumf.	through thickness
Tensile	modulus	GPa	25.5	46.9	-	35.9	37.2	-
	strength	MPa	44.8	31.0	10.1	86.9	77.2	13.0
Compressive	modulus	GPa	19.6	28.8	1.17	20.3	33.9	3.65
	strength	MPa	63.4	74.5	142	81.4	100	121
Flexural	modulus	GPa	24.1		-	32.4		-
	strength	MPa	71.7		-	124.8		-
Thermal	conductivity	W/mºK	274	246	104	209	199	129
	C.T.E.	10^{-6}/ºK	0.3	0.4	10.9	0.3	0.5	4.3

Table 3: summary of measured thermo-mechanical properties of resin-impregnated 2D and 3D CC brake materials.

Comparing Table 3 with Table 2, we note that the measured thermal conductivities of both 2D and 3D brake materials exceed the requirement for a machined thermal side by more than a factor of two. The Young's modulus is about as expected and the strength values are low.

The CTE is also low and well matched to quasi-isotropic face sheets made of high modulus graphite fibers.

9.2 Concept 1: Complete Tray Proof of Concept Prototype

9.2.1 Design Details and Materials

Material selections for the Concept 1 tray were driven by a combination of engineering, analysis, and material availability for construction of a prototype. Table 4 summarizes the materials used in the prototype and the properties assumed in the model of Section 10. Although the material choices listed in the table are considered adequate, further optimization of those choices will be conducted in Phase II with regards to stiffness and cost, primarily.

Component	Material	spec. mass (kg/m^3)	tensile modulus (GPa)			CTE (10^{-6}/ ºK)			thermal conductivity (W/mºK)		
			E_x	E_y	E_z	α_x	α_y	α_z	k_x	k_y	k_z
Face sheet	XN80/RS3 unitape [0/90/90/0], 200 μm	1779.2	239	239	-	-1.1	-1.1	-	130	130	0.1
Main core	YLA Cellular ULTRACOR UCF-130-3/8-0.7 [YSH70 ±45]	13.0	*.110*[a]	*.066*[a]	.041	-1.0	-1.0	-1.0	0	0	0
Closeout "C" channel	YSH50/RS3 plain fabric, [45/45], 250 μm	1666.5	8.1	8.1	-	-0.4	-0.4	-	27	27	0.1
Thermal wall	3D CC impregnated brake material	1800.0	35.0	35.0	3.5	0.4	0.4	4.3	200	200	130
Thermal wall core	YLA Cellular ULTRACOR UCF-83-1/4-2.5 [XN50 ±45]	40.0	*.483*[a]	*.276*[a]	0.552	-1.0	-1.0	-1.0	0	0	0
Corner/side clips	3D CC impregnated brake material	1800.0	30.0	30.0	1.2	0.4	0.4	10.9	308	308	104

[a] for cores, shear moduli G_x and G_y are listed instead of tensile moduli E_x and E_y

Table 4: material properties (partial list) used in FE model of Concept 1 closeout; note that the core listed in the table was not available in time for Phase I so that a much heavier GFRP fabric core was used instead).

The "C" channels were molded from two layers of YSH50/RS3 0/90 balanced plain fabric prepreg. Both layers were angled at 45 degrees to maximize shear stiffness in the "web" of the "C" between the face sheets. Figure 19 shows photographs of one of those channels. The YSH fabric is a thin (125 micron per layer) woven fabric of relatively high modulus but low cost fibers. The RS3 resin (from YLA) is a space qualified cyanate ester with very low outgassing and moisture absorption.

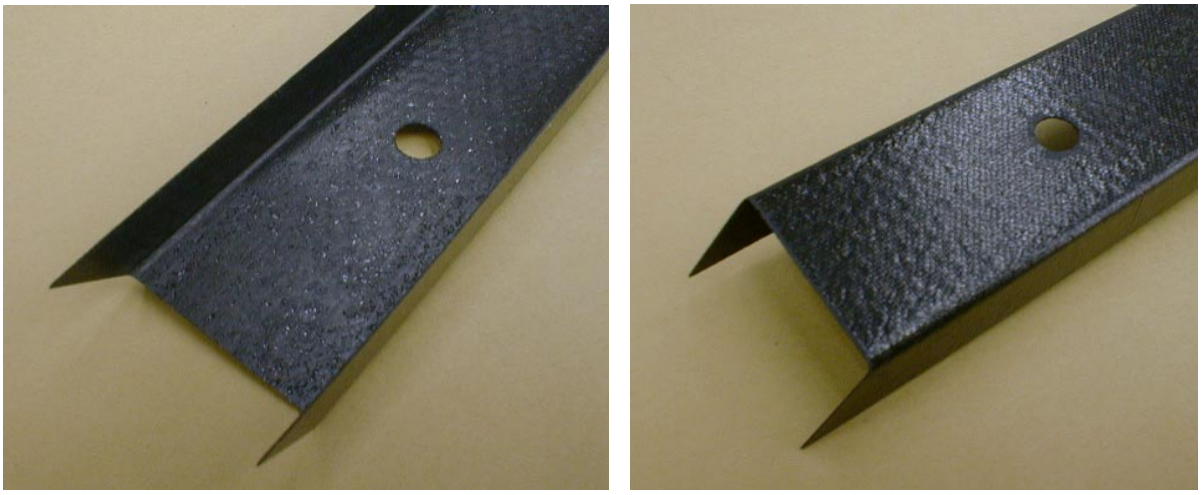

Figure 19: thin shell carbon fiber / cyanate ester resin "C" channel ready for assembly as part of concept 1 tray prototype.

The face sheets were molded from XN80/RS3 unidirectional prepreg tape. To keep the thickness to a minimum, a 4-layer, symmetric laminate of 0 and 90 degree plies was selected. A high-end fiber (XN80, 785 GPa modulus) was selected to maximize the stiffness to mass ratio. The same cyanate ester resin system was used (RS3). Figure 20 includes a photograph of the two face sheets.

To minimize multiple scattering and CTE mismatch issues while maximizing stiffness to mass ratio, graphite fiber honeycombs were used for both the main sandwich core and the thermal wall backing core. Lightweight fabric cores were obtained from YLA Cellular, Inc. They are shown in Figure 20. Note that much lighter weight honeycombs yet are being developed by YLA Cellular and will be considered for Phase II.

Figure 20: Left to right: main GFRP honeycomb core, GFRP face sheets, and side/filler core.

To achieve high thermal conductivity into the tower sidewalls, the two thermal sides were CNC machined from resin impregnated 3D C-C brake material. As shown above, this material exhibits thermal conductivities in all directions well in excess of the requirement for this application. All brackets (corner and side) were machined from impregnated 2D C-C brake material. These components are illustrated in Figure 21 and Figure 22. Note that the heat transfer boss is created as part of the finish machining operations on the completed tray.

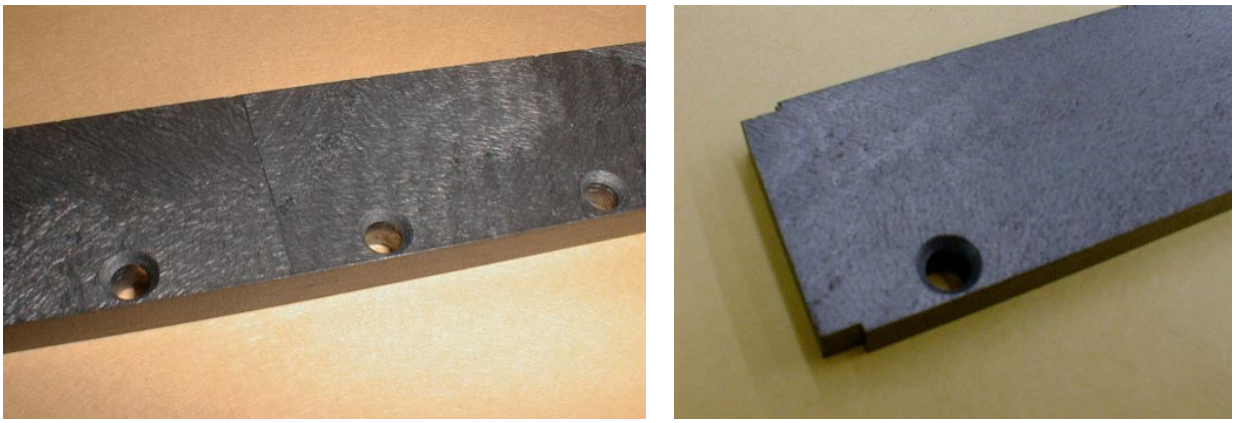

Figure 21: solid 3D CC thermal wall piece before assembly into concept 1 prototype; the deep recess for the PC boards is machined after assembly, removing most of the material.

Figure 22: corner (left) and center (right) clips used for concept 1 tray prototype; the parts were made of 2D CC; left view also shows one of the metal inserts to be bonded and later drilled and threaded.

All C-C parts receive metal inserts for bolted connections with the tower sidewalls. In this proof of concept prototype, we used 6061-T6 aluminum bar stock to machine those inserts. We are considering the use of other metals (titanium, beryllium) in Phase II. One such insert is visible in Figure 22; note that to insure close positional tolerances, the threaded holes are also machined after the entire tray is completely assembled. Bonded metal inserts are also used for the eight corner posts.

9.2.2 Fabrication Process

In general terms, the fabrication process consists of three phases:

1. Prepare (mold and machine) all components of the tray and bond blank metal inserts.
2. Bond all components together using precision fixtures with room-temperature glues.
3. Machine all critical features (outer surfaces, threaded holes, alignment faces and holes in corner posts) on the finished assembly.

Some of those steps are illustrated in the Figure 23. The bonding operations are facilitated by the use of specially made fixtures that provide both the alignment and the clamping pressure during bonding operations. A precision-machined aluminum base plate and two sets of aluminum bonding bars were used to assemble the prototype. To minimize the risk of distortion and residual stresses, all bonding was done with room-temperature-cured epoxy adhesives.

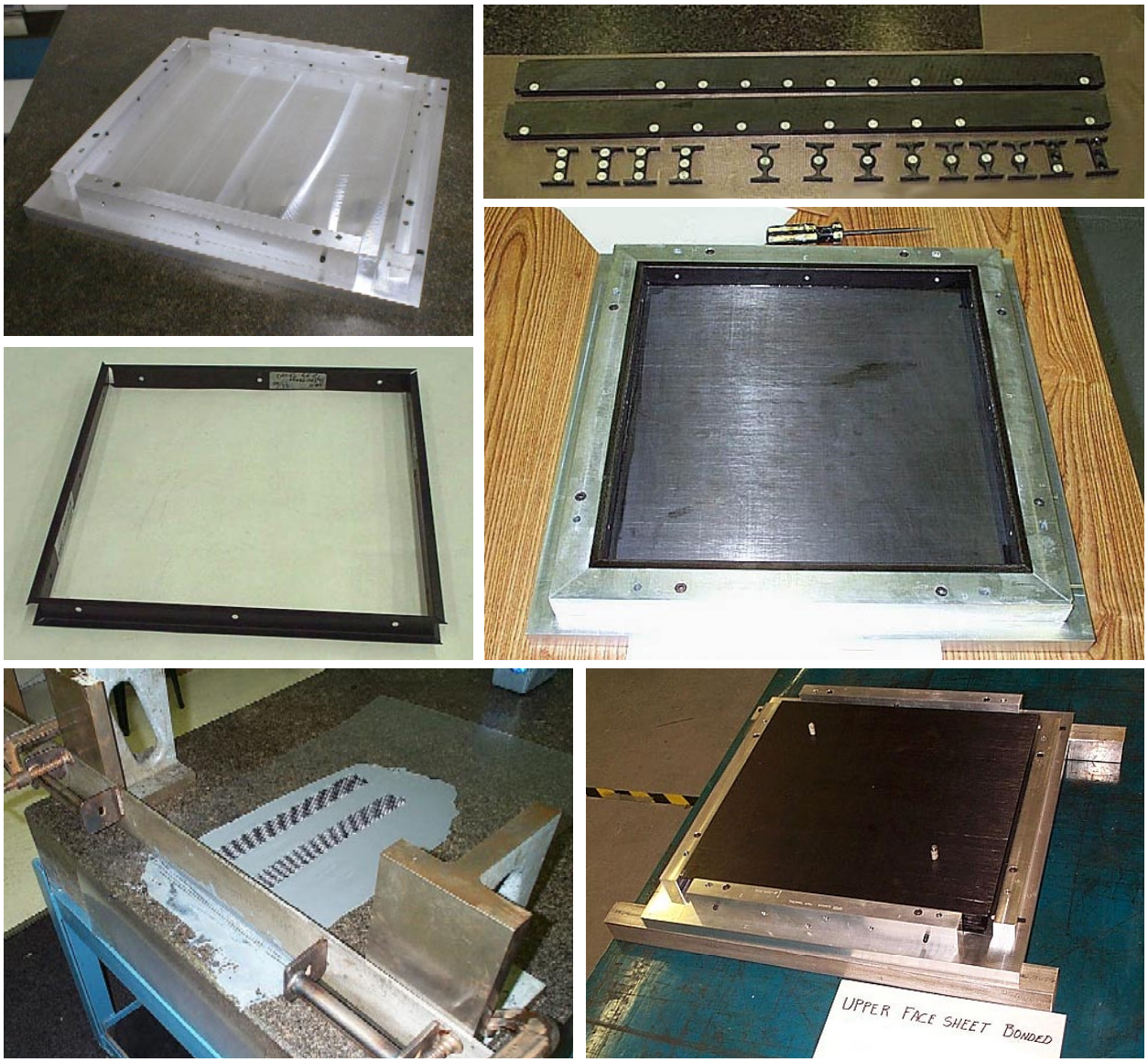

Figure 23: Various assembly steps of Concept 1 composite tray prototype; left to right and top to bottom: the bonding fixture with locating features for thermal sides and brackets, bonding metal inserts into thermal sides and brackets, the 4 'C' channels ready to bond, bonding the 'C' channels to the bottom face sheet, dipping the side cores to minimize the amount of glue, bonding brackets and thermal walls into 'C' channels.

When bonding honeycomb cores, a dipping process was used to apply adhesive only along the edges of the cell walls. This technique minimizes the amount of adhesive used (which is otherwise quite sizeable for an ultralight sandwich) and, once the proper procedure and adhesive viscosity has been found, provides very high quality bonds with good wetting of both the core walls and the face sheets.

9.2.3 Finished Prototype

After completion of all bonding operations, all critical features are CNC machined on the completed tray. This insures tight tolerances on final dimensions without requiring extreme accuracy in bonding. To maintain cleanliness, no lubricants are used in any of those machining operations. The entire prototype fabrication was quite successful and resulted in a very lightweight, stiff, and accurate tray assembly (Figure 24). The prototype is entirely made of graphite fiber reinforced composites, with the exception of the metal threaded inserts.

Figure 24: Finished concept 1 composite tray prototype.

Figure 25 shows a number of details of the concept 1 prototype tray; note the interlocking corner brackets and thermal walls, the metal inserts (now with threaded holes), the corner posts, and the recess in the thermal sides ready to receive the PC boards.

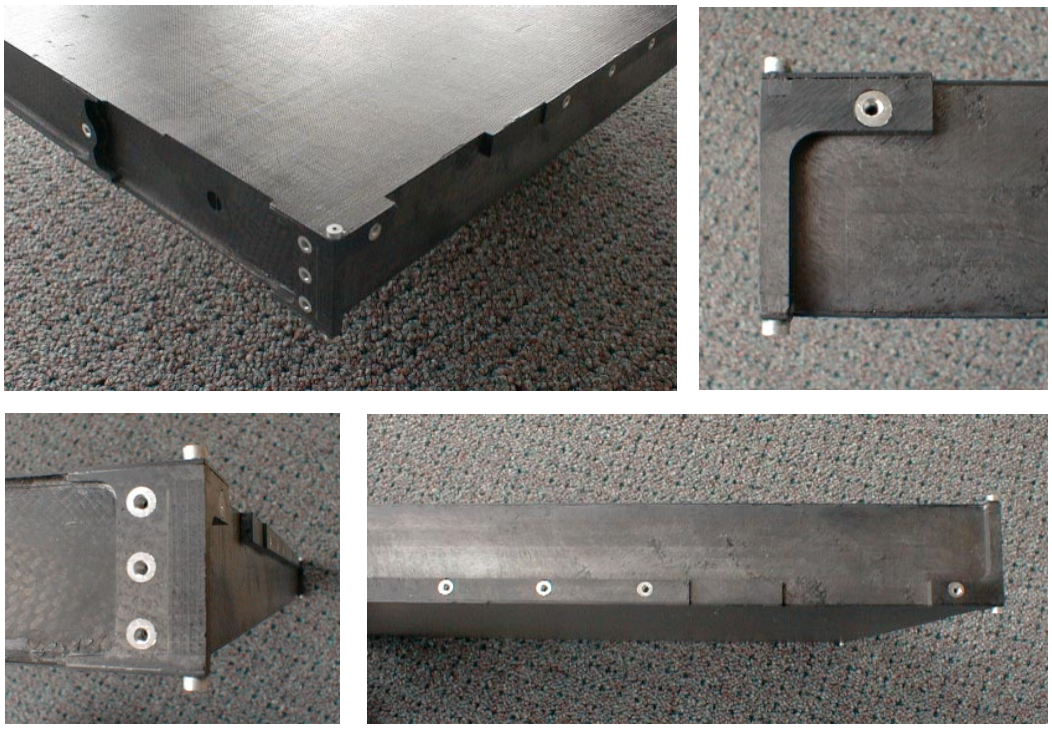

Figure 25: Details of concept 1 composite tray prototype.

This prototype will be the object of a series of dimensional, strength, and stiffness tests to be performed in Phase II of this SBIR.

9.2.4 Conclusions

The prototype Concept 1 tray produced in Phase I clearly demonstrated the feasibility of the approach. Final material selections will be refined in Phase II to further optimize mass, stiffness, radiation length, and cost. The assembly techniques and fixtures performed essentially as expected, although some refinements will be incorporated in future tools to accelerate the bonding operations.

Because of the reliance on final machining at the assembly level to achieve close tolerances, fresh C-C material is exposed on most lateral surfaces of the closeout. To minimize the risk of release of carbon micro-particles, this will likely require the development of a surface coating technique that can be applied to all sides of the closeout as the very last step of fabrication. This is one of the major goals of Phase II.

9.3 Concept 2: Component Prototypes

Because the second closeout concept is not as tightly integrated with the fabrication of the tray itself, fabrication of a complete tray prototype was not judged necessary. Instead, prototypes of a number of key elements of the concept were fabricated; these include the structural thin-wall tube, the three concepts for the thermal sides (Figure 14), and the corner pieces.

9.3.1 Fabrication of structural tubes and 2- and 3- piece thermal side concepts 2.b and 2.c.

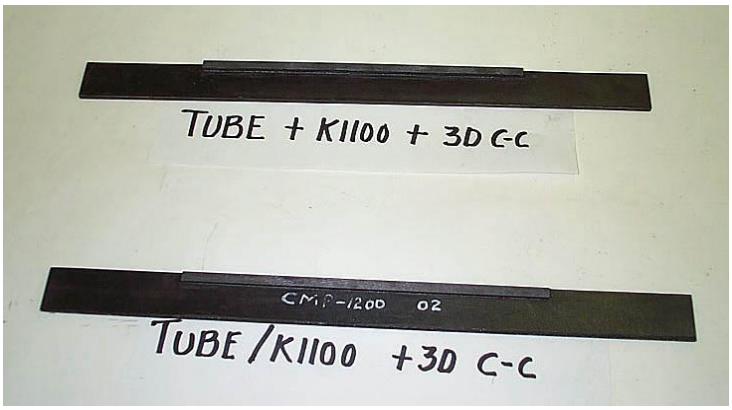

Figure 26: Prototype Concept 2.b (above) and 2.c (below) thermal sides: top piece is made from GFRP thin wall tube with post-bonded K1100 GFRP thermal backplane and 3D CC thermal boss bonded with thermally conductive epoxy; bottom piece is similar but has the K1100 layers co-cured with the thin wall tube.

Four structural thin walled tubes were produced in Phase I. The tubes were molded by wrapping two +/-45º layers, each approximately 150 μm, of YSH50/RS3 plain weave balanced fabric prepreg inside and outside of two 0º layers of YSH50/RS3 unidirectional tape prepreg, each around 50 micron thick, around a smooth chromed steel mandrel. The tube is then pressed in a rubber female mold and cured at elevated temperature, and the mandrel is forced out of the cured tube. The resulting composite tubes were of good quality and without measurable bow.

Two of those tubes (Figure 26) were modified to become thermal sides prototypes as described in Section 7.2, concepts 2.b and 2.c.

The first approach (2.b) consists of bonding a precured sheet of K1100/RS3 composite (4 layers, symmetric, + and - 70º angles from long axis) to one face of the precured structural tube with room temperature cured epoxy.

The second approach includes the four K1100 layers as part of the tube laminate, before cure. Those layers are then cocured to the structural layers in one step. The risk here is to induce bowing in the finished tube because of the CTE differential between the two fiber systems. The prototype, however, did not exhibit measurable bow.

In both cases, a machined 3D C-C heat transfer boss is then bonded to the K1100 side with a thermally conductive room temperature cured epoxy (Master Bond EP21TCHT-1, 1.44 W/mK).

9.3.2 Fabrication of thin CC shell tube (2.a)

We also attempted to produce several prototypes of the thin CC shell thermal side described earlier. The shells are made from a P30 unitape precursor that is molded around a steel and low melting alloy mandrel. The main rectangular portion of the cross section is formed by the steel mandrel, while the shorter thermal boss is wrapped around a low melting alloy mandrel. The assembly is cured at elevated temperature, and then heated to a higher temperature

to melt the secondary core. The main steel core is then pulled out and the shell is carbonized then densified by CVD.

This fabrication approach is far from straightforward, and a number of difficulties had to be worked out. First, laying up the prepreg layers around the very tightly curved corners of the cross sections takes practice; initial attempts resulted in wrinkling of the plies when the assembly was pressed in a female mold during cure.

Selection of the low temperature alloy used for the secondary mandrel also required some trial and error experimentation. Initial tests showed significant softening of that mandrel during cure. Selection of a higher melting point alloy largely eliminated this problem.

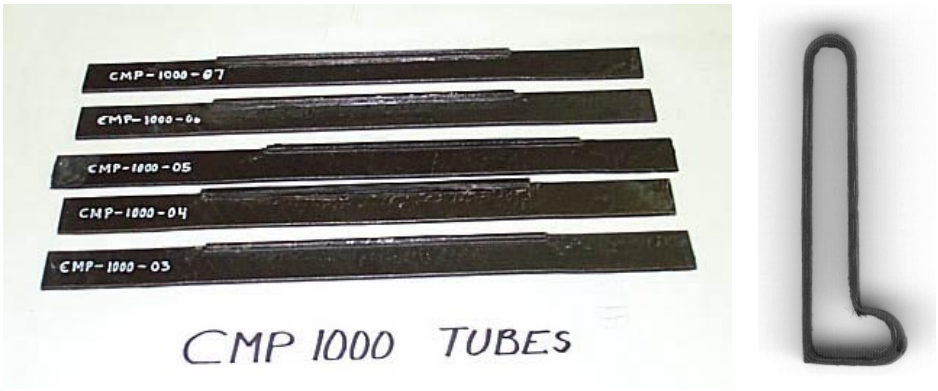

Figure 27: Prototype Concept 2.a thermal sides: single piece molded CC thin wall shells with integral heat transfer boss.

The final few prototypes started to exhibit better geometric tolerances (although still far from acceptable) and did not present any major flaws. A few of those are shown in Figure 27; the cross section in the right hand side shows a reasonable quality, with uniform wall thickness and fairly controlled geometry. However, the outer surface of the heat transfer boss is still much rounder than desired. Improvements in tooling (female cavity molds) could potentially help with this aspect.

9.3.3 Corner Pieces

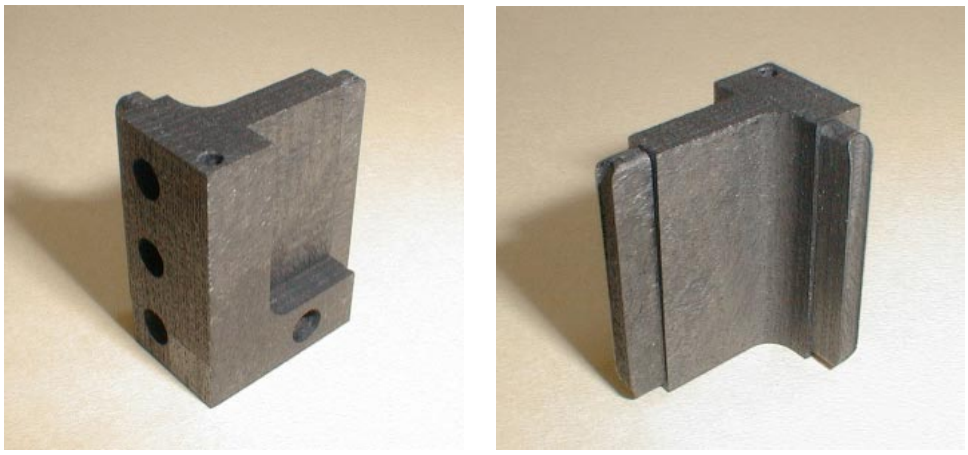

Figure 28: Prototype Concept 2 corner piece, milled from resin impregnated 3D CC brake material.

Corner pieces for the second concept were CNC machined from thick resin impregnated C-C brake material. A finished part is shown in Figure 28. The machining is very straightforward, owing to the self-lubricating property of C-C. Dimensional accuracy, stability, and surface finish are all excellent.

9.3.4 Conclusions

The prototyping of concept 2 components confirmed feasibility of the "picture frame" approach to building a closeout. Thermal sides can be easily produced by either co-curing or secondary bonding high conductivity layers to a molded structural thin wall tube. The resulting tubes are almost perfectly straight with good quality flat faces for heat transfer.

The C-C monolithic thin shell approach to the thermal wall fabrication proved less successful: although continuous progress was made from each prototype to the next, the final prototypes still show lack of control of the cross section geometry. Given enough development effort, the approach appears feasible, but it cannot be considered a viable, cost effective option for this application.

10. FE Modeling of Concept 1 Tray Assembly

10.1 Model Description

A finite element model of the concept 1 tray was constructed in the COSMOS[11] finite element analysis package. The model includes all components of the assembly, using orthotropic, multi-layered material property definitions. The level of detail is sufficient for accurate predictions of static deflections and dynamic behavior, and useable for rough estimation of stress levels.

The model contains more than 5900 solid brick and composite shell elements. Attachment to the tower sidewalls and neighboring trays are simulated with a set of boundary conditions on the closeout. All nodes at attachment bolts with sidewalls are allowed to move

only in a direction orthogonal to the wall (neglecting bending reactions from the side walls), and nodes at the top and bottom corner posts are restrained in the vertical direction.

Because in particle detectors like GLAST the tray payload (converters, bias circuits, and silicon detectors) contributes the major part of the total mass as well as a significant portion of the stiffness, all payload layers were also included in the model. The current GLAST design baseline was used in that model: 4x4 array of 400 micron thick silicon strip detectors bonded to a Kapton/copper flexible bias circuit, itself bonded to a 4x4 array of 3.5% lead converter sheets (bottom only). The bias circuit, converters, and glue layers are modeled as additional layers of the corresponding face sheet, while the detector ladders and edge bonds are modeled using a separate layer of isotropic shell elements. Note that this modeling technique has been validated against experimental modal tests performed on prototype GLAST trays.

10.2 Dynamic Behavior

On of the most important requirements for a tray assembly is that its lowest natural mode should be stiff enough to avoid collisions between neighboring trays in a tower, when excited by random vibrations. This requirement can be reduced to a minimum value for the fundamental frequency of the tray of approximately 500Hz.

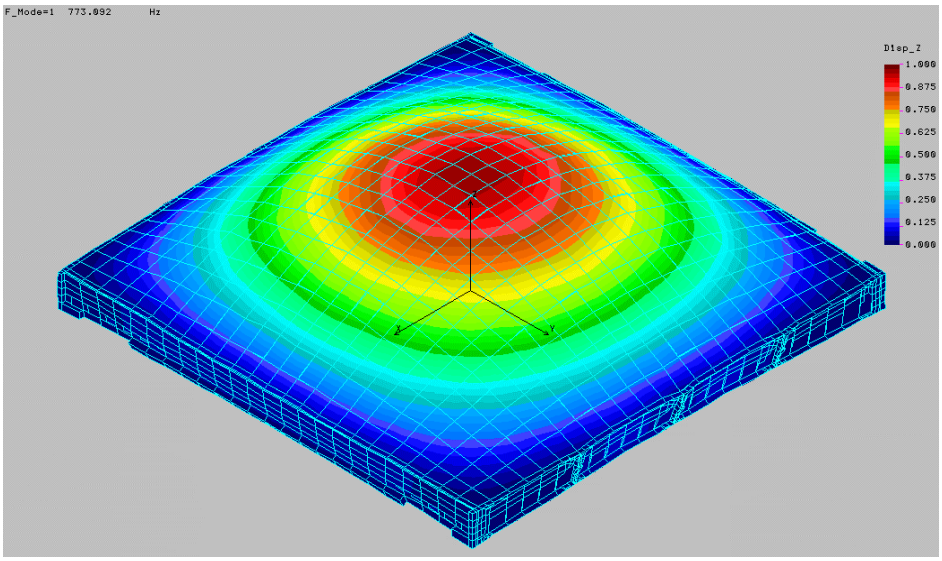

Figure 29: fundamental vibration mode (773 Hz) of the composite tray (concept 1); boundary conditions mimic attachment to thin, flexible side walls.

Figure 29 shows the fundamental tray mode as predicted with the COSMOS model; the predicted frequency is about 770Hz, comfortably above the required value, leaving plenty of room for further design refinement in Phase II.

10.3 Static Response

The static responses to the two design load cases defined in Section 5 were calculated with the model. The static deflections of the tray (Figure 30 and Figure 31) are very small for both load cases: less than 3.5 micron.

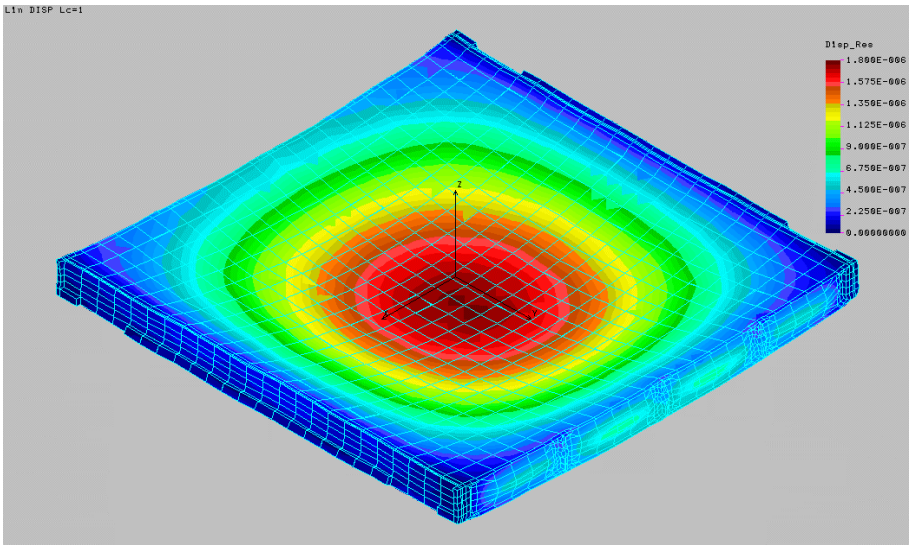

Figure 30: Static response of Concept 1 composite tray to Liftoff/transonic limit loads (3.35gZ + 4gY); color code shows the displacement resultant in meters; maximum displacement is about 1.8 micron at the center of the tray.

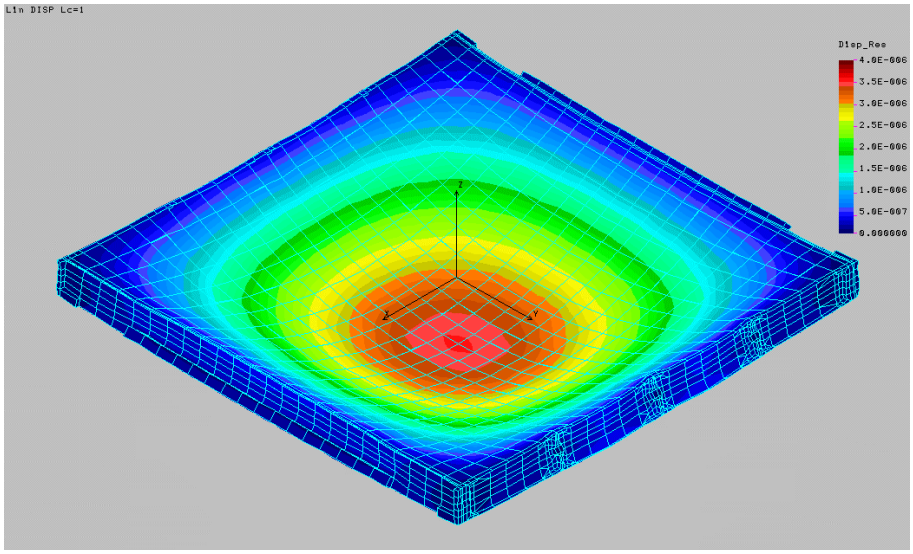

Figure 31: Static response of Concept 1 composite tray to MECO limit loads (6.6gZ + 0.1gY); color code shows the displacement resultant in meters; maximum displacement is about 3.5 micron at the center of the tray.

As mentioned before, the tray design is clearly stiffness driven. Because of this, stress levels are generally low throughout the tray structure. Figure 32 shows two locations in the closeout (the side brackets and the thermal sides) that experience the largest stress components. Even there, the peak uniaxial stress levels are less than 400kPa. This is more than two orders of magnitude smaller than the measured strength of C-C brake materials, 30 to 100 MPa.

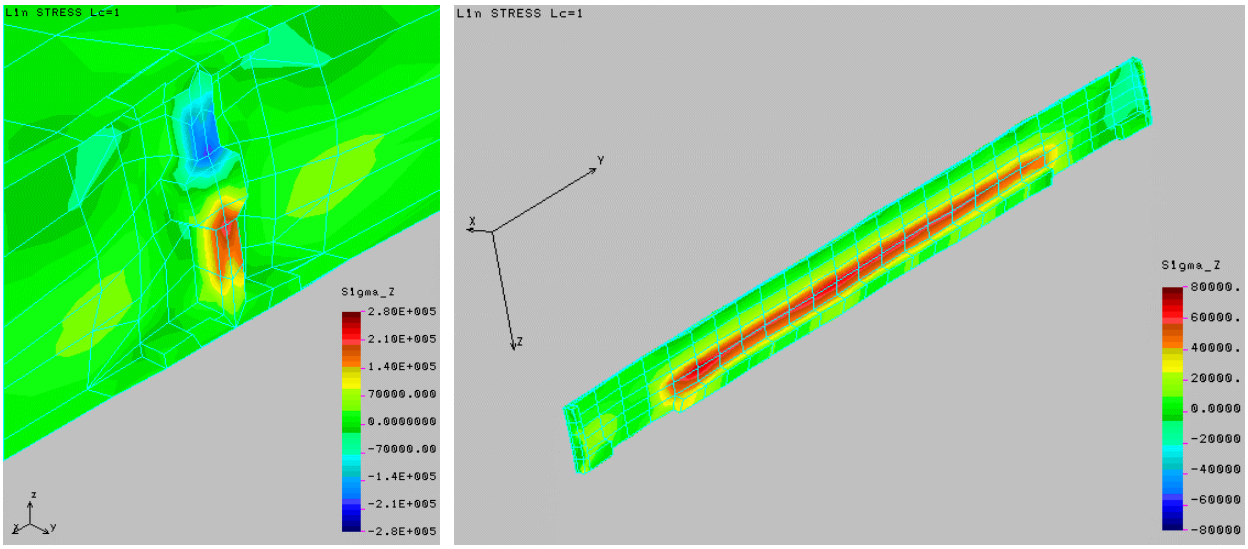

Figure 32: Static response of Concept 1 composite tray to MECO limit loads (6.6gZ + 0.1gY); left view shows largest uniaxial stress (0.28 MPa) in side clip; right view shows largest uniaxial stress in thermal wall (70 kPa); stress levels at other locations in the tray are less than 50 kPa.

10.4 Thermal Stress Issues

As discussed earlier, thermal stresses resulting from CTE mismatch between tray and payload components are a potentially serious issue for large area silicon detector systems. The FE model can be used to predict stresses and deformations in the tray and payload assembly, in response to a uniform temperature change.

As a point of reference, Figure 33 (previously shown in Figure 8) shows the distribution of membrane, ladder direction stress (σ_X) in the silicon detectors for a baseline aluminum closeout tray subjected to a +20ºC temperature change from room temperature (the assembly is assumed free of residual stresses at room temperature). The peak stresses exceed 10MPa (1450 psi) and occur in the ladders running along the edges of the tray because of substantial deformations of the tray in those areas, as shown in Figure 8 (due to CTE mismatch between the aluminum closeout and the rest of the assembly). Note that at the other extreme of the survival range (-20°C), the temperature differential and the stress levels are double those of Figure 33, more than 20MPa (2900psi). Although the strength of silicon detectors is quite variable depending on manufacturing parameters (particularly the quality of the dicing), some large silicon strip detectors have been known to fracture at stress levels as low as 3000psi. Note also that in addition to the risk of brittle fracture of the chips themselves, the conductive bonds used to attach the detectors to the bias circuits will also experience very high shear stress levels.

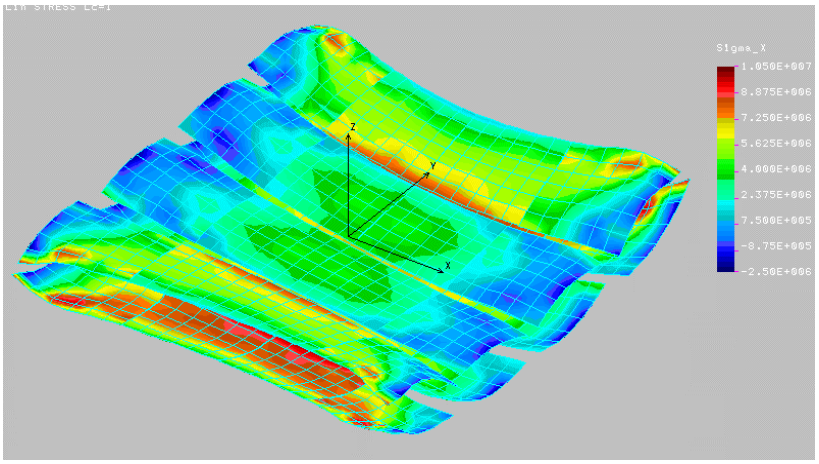

Figure 33: Static CTE-induced response of baseline tray assembly with aluminum closeout to a uniform +20°C temperature change from 20°C (assembly temperature) to 40°C (upper limit of survival range); for clarity, only the silicon detectors are shown; color code shows uniaxial stress in the ladder direction in Pascals.

The same calculations were performed for the concept 1 tray developed in this project. Those results are illustrated in Figure 34, where ladder-direction thermal stresses (σ_X) and out-of plane deflections (u_Z) in the silicon detectors are shown. With the carbon composite closeout, the thermal stresses are reduced by more than 60%, to below 4MPa (580 psi) for a +20°C temperature change. At the cold end of the survival range, this would translate into less than 8MPa (1160 psi), a much safer level. Note that much of that stress is due to a CTE differential between the top and bottom face sheet and payload combinations on the tray. That mismatch is itself due to the presence of the converter layers on the bottom side only. Further reduction of thermal stress levels would require better CTE matching of the top and bottom payloads and/or decoupling of the converter layers with soft, compliant adhesives. These aspects are beyond the scope of this SBIR.

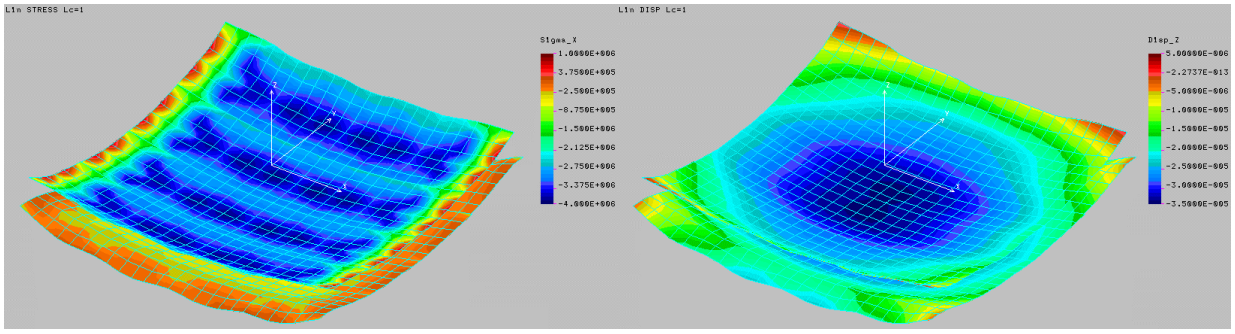

Figure 34: Static CTE-induced response of Concept 1 composite tray to a uniform +20°C temperature change from 20°C (assembly temperature) to 40°C (upper limit of survival range); for clarity, only the silicon detectors are shown; left view shows uniaxial stress in the ladder direction in Pascals, right view shows out-of-plane (Z) deflections in meters.

Another thermal response issue is the overall bowing of the tray that occurs once again because of the top to bottom mismatch in the payload layers. The model predicts a peak deflection at the center of the tray of the order of 35 micron for a +20°C temperature change. At the low temperature end of the survival range, this would again double to about 70 micron center deflection. Although such deflections are quite large, they are not believed to be a major issue because, in operation, the temperature within the tracker region would be much more stable (+/- a few degrees) than in survival mode.

11. Mass and Radiation Length Comparisons

For an instrument like the GLAST tracker, mass and percent radiation length budgets are extremely tight. Minimizing both of those properties then becomes a key goal in the design of the tracker structures. The masses and percent radiation length for closeouts and tray assemblies were evaluated for both composite closeout concepts from volumetric data extracted from 3D CAD solid models. Adhesives were approximately accounted for through engineering estimates. The results are summarized in Table 5 and Table 6 and compared to the baseline case of an aluminum closeout.

Table 5 compares mass and radiation length contributions from the closeouts alone. The masses of both composite closeout concepts are expected to be less than half the mass of the aluminum baseline. The percent radiation lengths are reduced by factors of 2.5 to 4.

Closeout Design	Total Closeout Mass		Area Averaged Normal Incidence ERL		Maximum Normal Incidence ERL	
	grams	% baseline	% RL	% baseline	% RL	% baseline
Aluminum Baseline	275	100	0.73	100	32	100
Composite Concept 1	128	47	0.20	27	12	38
Composite Concept 2	114	41	0.18	25	12	38

Table 5: comparison of mass and effective radiation length of carbon composite closeouts with baseline aluminum closeout.

In Table 6, we compare the baseline tray assembly (with aluminum closeout, aluminum honeycomb, and GFRP face sheets) to tray assemblies built with each composite closeout concept, an ultra-lightweight GFRP honeycomb core (much lighter than the core used in the concept 1 prototype), and a slightly thinner GFRP face sheet. With the added savings from the lighter core and face sheets, the mass is now reduced by more than 55% and the percent radiation length by more than 70%.

Tray Design	Face sheet	Core	Total Mass		Natural frequency	Area averaged normal incidence ERL	
			grams	% baseline	Hz	% RL	% baseline
Baseline	320 μm, XN50 [0/60/-60]s	Hexcel 3/8-5052-0.002-3	639	100	~ 800	1.49	100
Composite Concept 1	200 μm, XN80 [0/90]s	YLA Cellular UCF-130-3/8-0.7	279	44	~ 700	0.42	28
Composite Concept 2	200 μm, XN80 [0/90]s	YLA Cellular UCF-130-3/8-0.7	264	41	-	0.39	26

Table 6: comparison of mass and effective radiation length of various tray designs.

12. Other Issues

A number of important design issues that have not been considered in Phase I are listed below. All of these issues will be thoroughly examined and resolved in Phase II.

12.1 Protection of Composites Against Oxidation and Particulate Pollution

Probably the most critical issue with the concept 1 closeout is the amount of raw exposed machined carbon composites all around the closeout of the finished tray. Exposed graphite fibers and carbon matrix generate concern of electrically conductive carbon particles being released from these surfaces during assembly and launch, and re-depositing on critical electronic components or wire bonds.

To prevent this, it is likely that some type of surface coating will need to be developed to seal the exposed surfaces. That coating must be applied on the finished tray, after machining of all critical features is complete. This will likely reduce the available technological choices (chemical batch immersion may not be acceptable, for example). In addition, the coating must be sufficiently thin to not significantly affect thermal conductivity at the interfaces with the tower sidewalls, or dimensional accuracy of the critical alignment features. Both metallic coating (various techniques exist for deposition of such coatings) and simple resin coating will be considered.

12.2 Vacuum Outgassing of CC Materials

The substantial porosity of CC materials may cause difficulties with trapped gases that could be slowly released in orbit and cause contamination problems. The resin impregnation technique is expected to largely eliminate those concerns. However, careful testing of material samples will be required to qualify resin-impregnated C-C materials for space.

12.3 Mechanical Joints and Fasteners

In phase I, we used aluminum metal inserts for simplicity and machining convenience. Aluminum is clearly not a particularly good choice for small diameter threaded connections as it is quite susceptible to galling and plastic thread failure. As part of the phase II effort, other candidate materials will be considered, such as Titanium and Beryllium alloys.

13. Conclusions and Future Work

This Phase I project investigated conceptual design options for all-carbon-composite closeouts for space-qualified sandwich structures. Various approaches were considered and two promising concepts were further investigated through fabrication of component and assembly prototypes. In most cases, the prototyping efforts clearly demonstrated the feasibility of the proposed approaches. One concept in particular was shown to have significant advantages of simplicity and cost effectiveness. The concept is based on assembling the closeout from various simple components and does not require custom molding of complicated composite parts. The dimensional accuracy of the closeout is obtained by machining the entire assembly after all bonding operations are complete. The carbon composite closeout results in a 50% reduction in mass and more than 60% reduction in multiple scattering issues as compared to the previous design baseline.

A complete prototype of an all-carbon-composite tray based on that closeout concept was successfully fabricated in Phase I and did not reveal any fundamental difficulties. Further refinements to the assembly procedure and tooling should make the concept cost effective.

Finite element modeling of that tray concept confirmed the more than sufficient stiffness and strength of the proposed concept, as well as a substantial reduction in thermal stresses as compared to an aluminum closeout baseline.

In Phase II, a number of thermo-mechanical tests will be performed on that prototype to validate numerical predictions. Other issues related to qualifying the design for space will be investigated: these include particulate pollution from exposed carbon, outgassing of C-C composites, and final material selections (adhesives in particular). Additional prototypes will be built and tested for validation and qualification purposes. Finally, a complete tower of trays will be built and subjected to a complete set of qualification tests.

A successful Phase II continuation of the C-C closeout development program will lead to technology that will enable the use of machined C-C in primary load carrying thermo-structures for space applications. In particular, a technology for building closeout frames for ultra-lightweight, stable sandwich panels for space-based instruments would become available.

This new technology will immediately benefit the GLAST project by providing a composite closeout design that will be far superior to the current aluminum closeout design baseline:

- More than 50% savings in the mass of the closeout, leading to more than 44 kg saved on the instrument.
- Almost a 3 to 1 improvement in the effective radiation length of the closeout and the related multiple scattering issues.
- A very significant reduction in CTE mismatch and thermally induced stresses.

In March 2000, the Silicon-GLAST instrument was selected for the GLAST mission funded by NASA's office of Space and Science Strategic Plan, with a launch anticipated in 2005. The GLAST project has identified a composite material closeout frame as the baseline technology and a critical element of the tracker structures.

The successful development and qualification of the C-C closeout design will lead to a production order from the GLAST project for about 320 closeout frames for the GLAST instrument. Fabrication of those frames would start in July 2002, immediately after completion of the Phase II program (June 2002). It will be the first commercial implementation of the new technology in Phase III.

The implementation of the new carbon composite closeout technology in the GLAST project will also provide a key element of flight history that will be capitalized on in marketing the technology to other space programs.

14. Acknowledgments

In addition to SBIR funds, this work was partially funded under a collaboration agreement with the Stanford Linear Acceleration Center (Stevenson-Wydler CRADA # SLAC-183). The SLAC project manager for that portion of the work was Martin Nordby.

The authors wish to thank Wei Shih and Arturo Castillo, of Allcomp, Inc., for their invaluable support with this development project.

15. References

1. GLAST project web site at NASA GSFC, http://glastproject.gsfc.nasa.gov/
2. GLAST project web site at Stanford, http://www-glast.stanford.edu/index.html
3. GLAST Outreach web Site, http://www-glast.sonoma.edu/
4. General Environmental Verification Specification for STS & ELV Payloads, Subsystems, and Components (GEVS-SE), Rev. A, NASA Goddard Space Flight Center, June 1996.
5. Handbook of Composites, George Lubin, Ed., Van Nostrand Reinhold Co., New York, NY, 1982.
6. Structural Design and Test Factors of Safety for Spaceflight Hardware, NASA Technical Standard, NASA-STD-5001, June 21, 1996.
7. Designer's Reference Guide to Adhesive Technology, 3M, Industrial Adhesives and Aerospace Department, Industrial Tape and Specialties Division, 3M Center Bldg. 220-7E-01, St. Paul, MN 55144-1000, 1995.
8. Carbon-Carbon Composites, G. Savage, 1st ed., Chapman & Hall, 1993.
9. GLAST Science Instrument - Spacecraft Interface Requirement Document (SI-SC IRD) document, Rel. 0.4 (draft), NASA Goddard Space Flight Center, available from http://glastproject.gsfc.nasa.gov.
10. Draft thermal requirements for GLAST, Martin Nordby, SLAC, March 31, 2000.
11. COSMOS/M 2.5, finite element analysis package, Structural Research and Analysis Corporation (SRAC), Los Angeles, CA.